Folic Acid Deficiency Induces Premature Hearing Loss through Mechanisms Involving Cochlear Oxidative Stress and Impairment of Homocysteine Metabolism

Raquel Martínez-Vega[1,2], Francisco Garrido[1], Teresa Partearroyo[3], Rafael Cediel[1,2,4], , Steven H. Zeisel[5], Concepción Martínez-Álvarez[6], Gregorio Varela-Moreiras[3], Isabel-Varela-Nieto[1,2,7♦*], María A. Pajares[1,7♦]

[1]Instituto de Investigaciones Biomédicas Alberto Sols (CSIC-UAM), Arturo Duperier 4, 28029 Madrid, Spain,
[2]Unidad 761, Centro de Investigación Biomédica en Red de Enfermedades Raras (CIBERER), Instituto de Salud Carlos III, 28029 Madrid, Spain.
[3]Departamento de Ciencias Farmacéuticas y de la Salud, Facultad de Farmacia, Universidad CEU San Pablo, Boadilla del Monte, Madrid, Spain
[4]Hospital Clínico Veterinario, Facultad de Veterinaria, Universidad Complutense de Madrid, Avda. Puerta de Hierro s/n, 28040 Madrid, Spain.
[5]University of North Carolina at Chapel Hill, Nutrition Research Institute, Kannapolis, North Carolina, 28081 USA.
[6]Departamento de Anatomía y Embriología Humana I, Facultad de Medicina, Universidad Complutense de Madrid, Plaza de Ramón y Cajal s/n, 28040 Madrid, Spain.
[7]Instituto de Investigación Sanitaria La Paz (IdiPAZ), Paseo de la Castellana 261, 28046 Madrid, Spain.

♦These authors share senior authorship

*To whom correspondence should be addressed at: Institute for Biomedical Research "Alberto Sols" (CSIC-UAM), Arturo Duperier 4, 28029 Madrid, Spain. (Phone: 34-915854422; FAX: 34-915854401; email: ivarela@iib.uam.es)

Running head: Hyperhomocysteinemia and hearing loss

Abbreviations:

ABR: Auditory Brainstem Response

ADA: adenosine deaminase

ADK: adenosine kinase

AHCY: S-adenosylhomocysteine hydrolase

ARHL: age-related hearing loss

BHMT: betaine homocysteine methyltransferase

CBS: cystathionine β-synthase

DAB: 3,3'-diaminobenzidine

EDTA: ethylenediaminetetraacetic acid

GSH: glutathione reduced form

GSSG: glutathione oxidized form

Hcy: homocysteine

HL: hearing loss

HPLC: high performance liquid chromatograply

H&E: haematoxylin and eosin

MAT: methionine adenosyltransferase

MTHFR: methylenetetrahydrofolate reductase

MTR: methionine syntase

3-NT: 3-nitrotyrosine

PBS: phosphate buffered saline

PFA: paraformaldehyde

pHcy: plasma homocysteine

RT-qPCR: real-time reverse transcriptase polymerase chain reaction.

TUNEL: terminal deoxynucleotidyl transferase dUTP nick-end labeling

ABSTRACT

Nutritional imbalance is emerging as a causative factor of hearing loss (HL). Epidemiological studies have linked HL to elevated plasma homocysteine (pHcy) and folate deficiency, and showed that folate supplementation lowers pHcy levels potentially ameliorating age-related HL. The purpose of this study was to address the potential impact of folate deficiency in HL and to unveil the underlying mechanisms. For this purpose, two-month old C57BL/6J-mice (*Animalia Chordata Mus musculus*) were randomly divided in two groups (n=65 each) that were fed folate-deficient or standard diets for 8 weeks. HPLC analysis demonstrated 7-fold decline in serum folate and 3-fold increase in pHcy levels. Auditory brainstem recordings showed that only folate-deficient mice exhibited severe HL and cochlear $TUNEL^{+}$-apoptotic cells. RT-qPCR and Western-blotting showed reduced levels of enzymes involved in Hcy production and recycling, together with 30% increased protein homocysteinylation. Redox stress was evidenced by decreased expression of *Cat*, *Gpx4* and *Gss* genes, increased levels of the proteins MnSOD and the NOX-complex adaptor p22phox, and elevated concentrations of glutathione species. Altogether, our findings show for the first time that the relationship between folate-induced hyperhomocysteinemia and premature HL involves impairment of cochlear Hcy metabolism and associated oxidative stress.

Keywords: apoptosis, dietary restriction, hair cell loss, hyperhomocysteinemia, methionine cycle.

INTRODUCTION

Moderate-to-profound hearing loss affects over 360 million people worldwide according to recent World Health Organization data. Its incidence varies in each population segment, being approximately 10% in children, rising to 30% in adults over 65-years (age-related hearing loss, ARHL) and further increasing with age (1, 2). It is caused by a combination of genetic and environmental factors and has a tremendous impact in the quality of life of the elderly (2, 3). In contrast with congenital deafness, little is known about the genetic factors that contribute to ARHL, most of the available information deriving from the study of mouse models (4, 5). Regarding environmental factors, noise and ototoxic drugs are among the well-known stressors inducing early hearing loss (6, 7), but a few reports have suggested recently a role for the nutritional status in premature hearing impairment. Indeed, decreased levels of essential nutrients, such as several vitamins, have been shown to correlate with hearing loss (8-14). Among micronutrients, reduced folic acid concentrations have been found in ARHL and sudden sensorineural hearing loss, this decrease correlating with either reduced vitamin B12 status (11, 12) or increased homocysteine (Hcy) levels (13). Accumulating evidence from epidemiological research has shown the association between atherosclerosis in the inner ear and poor hearing, as well as the relationship between risk factors of vascular disease and ARHL (15-17). The intimate relationship between Hcy, an independent risk factor for cardiovascular disease, and folic acid metabolism provides the basis by which supplementation with the vitamin lowers plasma Hcy levels (18), an intervention that has been reported to ameliorate ARHL in a randomized trial (19).

Hcy constitutes a metabolic branchpoint linking the methionine and folate cycles and the trans-sulfuration pathway (Figure 1A). Hcy remethylation is catalyzed by either cobalamine-dependent methionine syntase (MTR) or betaine homocysteine methyltransferase (BHMT), enzymes that use 5'-methyltetrahydrofolate and betaine as methyl donors, respectively (20). Both reactions generate methionine that is in turn used to synthesize S-adenosylmethionine, the main methyl donor for cellular transmethylations. Donation of the methyl group renders S-adenosylhomocysteine that is hydrolyzed by S-adenosylhomocysteine hydrolase (AHCY) to Hcy and adenosine in a reversible reaction. Elimination of Hcy takes place by conjugation with serine in a B6-dependent reaction catalyzed by cystathionine β-synthase (CBS), or by export into the plasma. The correct function of the pathway depends on a continuous supply of 5'-methyltetrahydrofolate that is recycled in the folate cycle, where

methylenetetrahydrofolate reductase (MTHFR) exerts a key role. Epidemiological studies have analyzed the putative relationship of the *MTHFR* C677T mutation with hearing loss with contradictory results (21-23). Animal models have also generated data that, collectively taken, support a central role for Hcy metabolism in hearing pathophysiology. For example, *Cbs*$^{+/-}$ mutant mice have increased hearing thresholds, high concentrations of Hcy in the stria vascularis and the spiral ligament, oxidative stress and reduction of vessel density, effects that were prevented by the administration of folic acid in the drinking water (24). Hearing impairment has been also described in *Connexin 30* (*Cx30*$^{-/-}$) null mice, where the stria vascularis exhibited down- and up-regulation of *Bhmt* and *Ahcy* expression, respectively, and elevated levels of Hcy immunostaining (25).

Altogether human epidemiology and mouse genetic data reinforce the hypothesis that folic acid deficiency and Hcy metabolism play an important role in hearing disorders, although the mechanisms by which cochlear function is affected remain poorly understood. Here, we have used a rodent model of folic acid deficiency (26, 27) to show that a reduced intake of this essential vitamin causes cochlear impairment of Hcy metabolism, oxidative stress, severe cellular damage and apoptotic cell death leading to accelerated hearing loss.

MATERIALS AND METHODS

Mouse handling and experimental design

Two month-old C75BL/6J female mice were purchased from Harlan Interfauna Ibérica S.A. (Barcelona, Spain) and housed under standard conditions. The C57BL/6J mouse strain is a well-characterized model of progressive HL due to the *Ahl* alleles present in its genome that shows ARHL from the age of six-months onward (28, 29). Mice were randomly divided into two experimental groups (n=65 each) that were fed different types of diets *ad libitum* for 8 weeks. The normal folate group (NF) received a maintenance diet containing standard folate levels (A04/A04C/R04, Scientific Animal Food & Engineering, Panlab, Cornellá de Llobregat, Spain), whereas the folate-deficient group (FD) received a folate-depleted diet (folic acid ≤ 0.1-0.2 mg/kg) as previously described (26, 27). At least 6 different mouse cohorts including both experimental groups were studied independently. All experiments were approved by the CSIC Bioethics Committee and carried out in full accordance with the guidelines of the European Community (2010/63/EU) and the Spanish regulations (RD 53/2013) for the use of laboratory animals. Additionally, certain experiments required the use of the *Bhmt*$^{-/-}$ null mice previously described (30), as specified below.

Hearing assessment

Hearing was evaluated by Auditory Brainstem Response (ABR) analysis to broadband click and 8, 16, 20, 28 and 40 kHz pure tone frequencies recorded at an intensity range from 90 to 20 dB SPL in 5-10 dB steps, as previously reported (31-33). Mice were anesthetized with ketamine (100 mg/kg) and xylazine (10 mg/kg). The electrical responses were amplified and averaged to determine hearing thresholds for each stimulus. Peak and interpeak latencies were analyzed at 15-20 dB SPL above hearing threshold after click stimulation. The FD group showed either moderate or profound hearing loss in two well-defined populations. Therefore, further determinations in the FD group were restricted to those animals exhibiting profound hearing loss.

Blood and tissue extraction

Mice were sacrificed by CO_2 asphyxiation for fresh tissue removal, and the isolated tissues were immediately frozen in liquid nitrogen for protein or RNA extraction. Blood samples were collected by cardiac puncture and directly placed in either regular or heparin (Laboratorios Farmacéuticos Rovi, Madrid, Spain) coated

tubes, centrifuged at 2500 xg for 10 minutes, and the respective serum and plasma fractions isolated and stored at -80ºC until use.

For histological analysis, mice were injected with a pentobarbital overdose and perfused with cold PBS and 4% (v/v) paraformaldehyde (PFA; Merck, Darmstadt, Germany). Cochleae were then dissected out from the temporal bone as previously described (34, 35). Isolated tissues were immediately frozen in liquid nitrogen or fixed for immunohistochemistry studies. Fixation was carried out overnight in 4% (v/v) PFA at 4ªC followed by decalcification with EDTA (Sigma-Aldrich, Tres Cantos, Madrid, Spain) for 10 days (31, 32). Decalcified samples were dehydrated and embedded in paraffin wax (Panreac Química, Castellar del Vallés, Barcelona, Spain) or cryoprotected in sucrose, embedded in a sucrose/gelatin solution and frozen in isopentane at -80ºC as previously described (36).

Cochlear Morphology and Immunohistochemistry

Cochlear cytoarchitecture was evaluated using representative paraffin sections (7 μm thick) stained with haematoxylin-eosin (H&E; Sigma-Aldrich) and Masson´s Trichrome (Sigma-Aldrich). Phalloidin histochemistry was performed on frozen sections using Alexa-488 conjugated phalloidin (1:100 v/v; Molecular Probes, Eugene, OR, USA). For paraffin immunohistochemistry, slides were dewaxed, rehydrated and the endogenous peroxidase inactivated for 20 minutes with 3% (v/v) hydrogen peroxide (Merck). For immunohistofluorescence, cryostat frozen sections (15 μm) were prepared using Cryocut 1900 (Leica Microsystems, Dearfield, IL, USA). All slides were permeabilized in 0.05% (v/v) Triton-X-100 (Calbiochem, LaJolla, CA, USA) in PBS (T-PBS) and non-specific tissue-binding sites were blocked for 40 minutes using 5% (v/v) normal rabbit or donkey serum (Sigma-Aldrich) in PBS. Samples were incubated with the primary antibodies overnight at 4ºC, washed with T-PBS and incubated with the corresponding secondary antibody for 2 hours at room temperature (Table 1). Slides were then washed with T-PBS and covered with a tertiary extrAvidin® peroxidase-conjugated antibody for 90 minutes (1:200 v/v; Sigma-Aldrich). Immunodetection was carried out with 3,3'-diaminobenzidine (DAB; Sigma-Aldrich). When indicated, sections were dehydrated and mounted with Entellan (Merck) or Prolong Gold with DAPI (Invitrogen, Carlsbad, CA, USA). All brightfield images were obtained using an Olympus DP70 digital camera mounted on a Zeiss microscope. Immunofluorescence images were acquired in a confocal microscope (Leica TCS SP2, Wetzlar, Germany).

Photomicrograph acquisition and densitometry for 3-nitrotyrosine (3-NT) quantification were performed as reported, using a minimum of four animals per group (32). Freehand-delimited areas for the stria vascularis and the cochlear ganglion were used for the optical density estimation using ImageJ software v1.43m. Three consecutive serial slides were studied and, for each section, at least two pictures per structure were taken. The same procedure was carried out for myelin P0 and Kir4.1 immunohistochemistry quantification. The relative intensity/area ratio of the cochlear ganglion was performed on paraffin sections stained with H&E using ImageJ software. Every fifth slide was analyzed so that at least four representative sections for each animal and cochlear region were included.

Metabolite determinations.

Total pHcy was determined after derivatization using the Reagent kit for the HPLC analysis of Hcy in plasma/serum (Chromsystems Instruments & Chemicals GmbH, Munich, Germany). Derivatized samples (50 µl) were injected into the HPLC column and fluorescence measured at 515 nm after excitation at 385 nm.

Plasma vitamin B6 levels were measured using a commercial kit (Chromsystems Instruments & Chemicals GmbH) and HPLC analysis coupled to fluorescence detection following manufacturer's instructions.

Total serum folate was determined using the microbiological method described by Horne and Patterson (37) with the modifications introduced by Tamura (38).

Reduced (GSH) and oxidized glutathione (GSSG) levels were measured by the method of Tietze as modified by Rahman et al. (39). For this purpose, two cochleae were homogenized in 0.1 M potassium phosphate buffer pH 7.5, containing 5 mM EDTA and 0.6% (w/v) sulfosalicylic acid (250 µl), centrifuged at 8000 xg 10 min at 4ºC and the corresponding extract used for GSH (1:10 v/v) and GSSG (1:2 v/v) determinations.

Protein extraction and Western blotting

Whole cochlear protein was prepared as previously reported (34, 40). Protein concentrations were measured using the Pierce BCA Protein assay kit (Thermo Scientific, Rockford, IL, USA) and bovine serum albumin as standard. Samples (200 µg) were loaded in 10% SDS-PAGE gels and electrotransferred for incubation with the corresponding dilutions of primary and secondary antibodies for 1 hour as specified in Table 1. Signals were developed using Western Lightning ECL (Perkin Elmer, Waltham, MA, USA). Blots were subjected to densitometric scanning using ImageJ and

the values normalized against α-tubulin or β-actin signals. Mean values for the NF group were considered 100%.

Real-time RT-PCR

Total cochlear RNA was isolated from NF and FD mice using RNeasy kit (Qiagen, Hilden, Germany), and the quality and quantity determined spectrophotometrically and by automated electrophoretogram on a Bioanalyzer 2100 (Agilent Technologies, Santa Clara, CA, USA). Reverse transcription and PCR were done as previously described using 1.25 μg of total RNA as template and the High Capacity Archive kit (Applied Biosystems, Foster City, CA, USA) (41). cDNAs (10 ng) were amplified in triplicate using gene specific primers (Table 2) and Power SYBR Green PCR Master Mix (Applied Biosystems) or TaqMan probes (*Cat, Foxm1, Foxp3, Gap43, Gclc, Gpx1, Gpx4, Gsr, Gss, Mef2a, Mef2d*), using the ABI 7900HT Real-Time PCR system (Applied Biosystems). Primers for *Cbs* and *Adk* amplification were designed to allow amplification of the two splicing forms of each gene reported to date. Fluorescent signals were collected after each extension step, and the curves analyzed with SDS 2.2.2 software. Relative expression ratios were normalized to the geometric mean of the *Rn18s* or the *Rplp0* genes. Experimental efficiencies were calculated for each transcript and used to obtain the fold changes according to Pfaffl et al. (42).

TUNEL assay

The presence of apoptotic cells was evaluated in cochleae using the ApopTag Plus Peroxidase In Situ Apoptosis Detection kit (S7100; Millipore Iberica S.A.U., Madrid, Spain) for TUNEL assay, according to manufacturer's instructions. Briefly, samples were fixed in PFA 1% (v/v) for 10 minutes at room temperature, washed twice in PBS and post-fixed at -20ºC in ethanol:acetic acid (2:1, v/v) for 5 minutes. Slides were then washed, endogenous peroxidase was blocked with hydrogen peroxide (5%, v/v 20 minutes), washed again and the equilibration buffer was added for 10 minutes. Next, samples were incubated at 37ºC for 1 hour with terminal deoxynucleotidyl transferase (TdT), and the reaction stopped and further incubated using the digoxigenin/anti-digoxigenin antibody system. The final reaction was monitored with a microscope using DAB as the chromogen. Afterwards, samples were dehydrated and mounted with Entellan (Merck). DNase I treated normal cochleae and rat post-weaning mammary gland tissue (S7115; Millipore) were used as positive controls, whereas negative controls were obtained by omitting the TdT enzyme. The number of TUNEL-

positive cells was evaluated as described above in four sections per animal (n=6 mice per group) and the resulting counts averaged for comparison.

Statistical analysis

SPSS v 19.0 software package (SPSS, Chicago, IL, USA) and GraphPad Prism v 5.0 (GraphPad Software, San Diego, CA, USA) were used for statistical analysis. Statistical significance was determined by Student's t-test for unpaired samples between NF and FD groups. All results are expressed as the mean ± standard error of the mean (SEM) and differences were considered significant when $p \leq 0.05$.

RESULTS

Plasma concentrations of selected metabolites were measured in mice receiving normal (NF) or folate-deficient (FD) diets in order to assess the effect of the treatment (Figure 1B). As expected, a severe reduction in serum folate levels (~7 fold) was observed in the FD group as compared to the NF group. Additionally, total pHcy concentrations were elevated (~3 fold) in the FD group, whereas plasma vitamin B6 levels were similar in both dietary groups. Hence, the diet was effective in causing systemic folate deficiency and hyperhomocysteinemia.

Folate deficient mice show early signs of severe sensorineural hearing loss.

Mice in the NF group had on average, normal hearing, whereas animals in the FD group had moderate (34%) or profound (66%) hearing loss; only the latter group was further studied and referred to as FD (Figure 2A-2C). An average increase of 45 dB SPL in ABR thresholds was found in FD mice when compared to the NF group in response to click stimuli. Accordingly, there was a significant increase in hearing thresholds at all studied frequencies, although the effect was more acute at high (50 dB SPL threshold shift) than at low frequencies (20 dB SPL threshold shift) (Figure 2C). Click ABR wave analysis revealed a significant delay in the latency of wave I in FD mice when compared to the NF group (Figure 2D), as well as a dramatic reduction of the amplitude of wave I (Figure S1A). No further differences were observed in ABR interpeak latencies (I-II, II-IV and I-IV) (Figure S1B) and the wave IV latency-intensity function when these parameters were measure at intensities of 20 dB SPL above threshold. However, a progressive decrease in the wave IV amplitude-intensity ratio was observed in the FD mice group (Figure S1C and S1D).

Folate deficient mice show aberrant cochlear cytoarchitecture and altered expression of cell-type markers.

Cochlear architecture differed between groups, with cellular loss in the basal turn seen in the FD mice, when compared to that in the NF group (Figures 3 and 4). The structure of the organ of Corti in the NF mice remained normal along all cochlear turns (Figure 3A, a-e). In contrast, the cochlea of FD mice showed a flat cochlear epithelium in the basal turn (Figure 3A, f-j). TUNEL-positive cells were evident in the organ of Corti and stria vascularis in the middle-turn of the FD cochlea, but not in the NF (Figure 3B and 3C). At the time studied, apoptotic cells were not observed in the flat basal turn or in the normal apex (data not shown). Additionally, other cellular populations were affected in the basal and middle turns of the cochlea of FD mice when compared to the

NF (Figure 4). Cellular aberrations included loss of type IV fibrocytes (compare Figure 4A and 4B with 4J and 4K) and a 33% reduction of ganglionar density and myelin P0 levels ($p<0.001$; compare Figure 4D and 4E with 4M and 4N and quantification in 4F, 4I and 4L). Myelin P0 levels remained unchanged for both dietary groups from the middle turn towards the apex (Figure 4L). Disorganization of the striatal capillaries and accumulation of melanin granules were also observed in 5 out of 9 mice of the FD group studied, in contrast, none of the NF group mice showed this phenotype (compare Figure 4G and 4H with 4P and 4Q; quantification in 4O and 4R). Kir4.1 levels did not show evident differences between the dietary groups ($p>0.05$; compare Figure 4G' and 4H' with 4P' and 4Q'). Furthermore, levels of genes expressed in the organ of Corti were analyzed (Figure S1E). *Mef2a* and *Mef2d* showed a small but statistically significant decrease in the FD group as compared to the NF, *Foxp3* levels were significantly increased ($p<0.05$) and there were no differences in *Gap43* and *Foxm1* levels.

Cochlear homocysteine metabolism showed specific expression features.

Systemic changes in folate and Hcy levels may reflect alterations in their cochlear metabolism, which has not been studied previously. Therefore, real-time RT-PCR (RT-qPCR) assays were carried out using cochleae of mice in the NF group to define the control expression pattern. (Figure 5A). Normalization of the results using the *Rn18s* housekeeping gene, and comparison of the calculated levels utilizing *Mat1a* data as reference, allowed identification of three transcript categories: 1) including *Mat2a*, *Mat2b*, *Ahcy* and *Adk* with levels >20-fold larger than those of *Mat1a*; 2) with intermediate expression levels (8-fold over *Mat1a*), comprising *Bhmt* and *Mtr*; and 3) with low expression levels of similar magnitude, integrated by *Mat1a*, *Ada*, *Cbs* and *Bhmt2*. These results confirmed the expected extrahepatic expression pattern, except for *Bhmt* and *Mtr* genes.

The corresponding proteins were detected by Western blotting, although differences in mobility (10-15 kDa) were found for BHMT and AHCY bands as compared to samples of liver origin (Figure 5B-D). In cochlear extracts, anti-BHMT and anti-AHCY detected proteins with calculated molecular masses of 68 and 58 kDa, respectively. In contrast, only a band of the expected mobility (~45 kDa) was visible when using hepatoma H35 cytosols, even when larger amounts of extracts or film overexposure were utilized. The specificity of the BHMT band was demonstrated by the lack of signal observed with either preimmune rabbit serum or cochlear extracts

obtained from *Bhmt*$^{-/-}$ null mice (Figure 5B and 5C). Again, the data demonstrate specific features of Hcy metabolism in the cochlea.

Folate deficiency induced impairment of cochlear homocysteine metabolism.

Systemic changes in folate and Hcy levels may reflect alterations in this part of cochlear metabolism. Therefore, RT-qPCR assays were carried out to analyze the putative changes induced by folate deficiency (Figure 6). The mRNA levels of enzymes involved in Hcy production (*Ahcy*) and remethylation (*Bhmt* and *Mtr*) reduced their expression in FD mice (30-50%), as compared to NF animals. In contrast, mRNA levels of enzymes involved in elimination of S-adenosylhomocysteine products showed no change (*Cbs* and *Adk*), or a tendency to increase (*Ada*; p= 0.08). In addition, no significant alterations in mRNA levels for *Mat* subunits were detected, neither were alterations detected for *Bhmt2*. Therefore, expression changes induced by folate deficiency were directed towards reduction of Hcy production and to favor its elimination to the plasma or through the trans-sulfuration pathway.

Cochlear expression levels however may not reflect the actual protein levels that were analyzed by Western blotting. Decreased protein levels were found in the FD group, as compared to NF samples, for the AHCY 58 kDa band (~40%), the double band ~60-65 kDa corresponding to CBS isoenzymes (~70%), and the BHMT 68 kDa band (~60%)(Figure 7A-C). In contrast, ADK (41 kDa) showed no change, whereas increased signals were found for the 138 kDa MTR band (~40%) and the 41 kDa ADA protein in FD cochleae (Figure 7D-F). This last protein gave no signal in NF samples. Again, the results suggest an effort to reduce Hcy production and towards elimination to the plasma. However, the combined effects on expression and protein levels in FD mice may not be enough to avoid the increase in intracellular Hcy levels. A consequence of such an intracellular enhancement of Hcy could be protein homocysteinylation, a protein modification that can be followed by Western blotting using total cochlear extracts and anti-Hcy (Figure 7G). The results indicated a 50% increase in immunostaining of FD cochlear proteins, as compared to NF extracts, indicative of cochlear hyperhomocysteinemia.

Folate deficient mice showed oxidative imbalance in the cochlea.

Hearing loss has been previously associated to redox imbalance, hence we next studied the putative effect of the FD diet on parameters of the cellular oxidative

response in the cochlea (Figure 8A). Protein levels of the NADPH oxidase complex (NOX4 and p22phox) and MnSOD were analyzed by Western blotting (Figure 8B). Similar NOX4 protein levels were found in both mouse groups, whereas a significant increase in p22phox (~1.5-fold) and MnSOD (~1.7-fold) levels were detected in FD cochleae as compared to NF samples. Expression levels of genes involved in redox control were also analyzed by RT-qPCR in both dietary groups (Figure 8C). Reduced transcript levels were detected for *Cat* (20%), *Gpx4* (30%) and *Gss* (15%) in the FD group, whilst no change was observed for *Gsr*, *Gpx1* and *Gclc* between dietary groups. GPX proteins require GSH and generate GSSG, hence cochlear glutathione levels were also determined. Increased GSH (60%) and GSSG levels (50%) were measured in FD as compared to NF samples (Figure 8D), but these changes did not significantly alter the GSH/GSSG ratio (7.76 ± 0.36 vs. 8.49 ± 0.56; $p=0.29$). A consequence of superoxide metabolism is 3-nitrotyrosine (3-NT) synthesis, a metabolite that can be immunostained in cochlear sections (Figure 8E). FD mice showed strong immunoreactivity for 3-NT in the stria vascularis and the cochlear ganglion, whereas mice on the NF diet exhibited low basal signals as described previously (43).

DISCUSSION

Hearing loss is one of the numerous health problems that appear associated with micronutrient deficiencies worldwide (8-13). Their origin relies not only in malnutrition, but also in an inadequate nutrient density in the so-called western societies. Among them, low serum and blood red cell folate levels have been detected in several types of hearing impairment, and in some cases an association with elevated pHcy concentrations also has been reported (11-13). However, the underlying mechanisms linking folate deficit and hearing loss remain unidentified. For this reason, we have used a nutritional mouse model that presents both with low serum folate levels and hyperhomocysteinemia, thus making it a suitable model for the analysis of the association of these alterations and hearing loss.

Evaluation of the auditory response shows higher thresholds with more acute losses at high frequencies in FD mice, hence demonstrating a direct association between folate deficiency, hyperhomocysteinemia and profound hearing loss. Wave I amplitude decrement confirms premature impairment at the hair cell auditory nerve synapse, similar to that described in hearing loss associated to oxidative stress (44). Histopathological analyses of hearing loss in FD mice indicate that different cochlear populations are affected. Severe damage was evident at the organ of Corti, the spiral ganglion, the stria vascularis and cells of the spiral ligament. Moreover, cochlear damage displayed a gradient, with severe cellular loss in the basal turn, signs of damage including the presence of apoptotic cells in the middle turn and very light or no phenotype in the apex. Differences in susceptibility against ototoxic drugs by cochlear cell populations are exhibited for example against treatments with salicylate (45) or cisplatin, a chemotherapy drug, which induces a larger loss of inner hair cells in the cochlear base than in the apex (46).

Folic acid is needed for Hcy remethylation, but knowledge of this part of cochlear metabolism was very limited, therefore requiring its characterization in control tissues. Most genes showed the expected expression profile for extrahepatic (high *Mat2a* expression) and non-lymphoid tissues (*Adk* vs. *Ada* expression) (47, 48). However, remethylation genes exhibited a specific pattern with similar expression levels for *Mtr* and *Bhmt*, and lower for *Bhmt2*, thus making the cochlea a different subtype among extrahepatic tissues. The corresponding proteins were also detected in immunoblots, commonly at very low levels. Anomalous mobilities for BHMT and AHCY bands, compatible with their post-translational modification, were also

observed, suggesting changes in their behavior and function. Large-scale mass spectrometry studies have detected a number of such modifications in these proteins (49), although their impact on BHMT and AHCY function has been scarcely explored (20).

Folic acid deficiency alters the cochlear gene expression pattern, reducing the expression of *Ahcy*, *Mtr* and *Bhmt*. Reduced *Bhmt* expression was previously described in the stria vascularis of *Cx30*$^{-/-}$ null mice, however in that model of hearing loss *Ahcy* showed a modest upregulation (25). This transcriptomic study did not report additional changes in genes of these pathways, neither were *Adk* mRNA or protein levels altered in rats exposed to broadband noise (25, 48). Expression results correlated with those of immunoblots for AHCY, BHMT and ADA, whereas levels of CBS splicing forms and MTR signals followed different patterns. Lack of correlation between mRNA and protein steady-state levels are not uncommon and may be due to changes in their half-lives. Consistent with this line of evidence, cobalamin-binding to MTR protein has been reported to stabilize this enzyme (50), an effect that could be expected in FD mice as an effort to recycle the low amounts of folate available. Altogether, changes induced by folic acid deficiency on Hcy metabolism are directed towards decreasing Hcy synthesis, (precluding the reversibility of the AHCY reaction through augmented adenosine utilization), reducing Hcy flux through remethylation and decreasing its use in trans-sulfuration. In this scenario, increased adenosine elimination may limit protection against cochlear oxidative stress through adenosine signaling (51), although sparing the purine for nucleic acid and NADH/NADPH synthesis. An additional drawback for cochlear function may derive from the reduced flux through trans-sulfuration. CBS and cystathionase are able to synthesize H_2S, whose protective role as cochlear vasodilator has been reported in noise-induced hearing loss (52). A reduced production of H_2S may contribute to the changes detected in striatal capillaries in FD mice, in concordance with the decreased vessel density previously reported for *Cbs*$^{(+/-)}$ mice cochleae (24).

Taken together the aforementioned alterations in Hcy metabolism suggest the presence of elevated Hcy levels in the cochleae of FD mice, an increase that is confirmed by detection of enhanced Hcy immunostaining along FD protein lanes. Increased Hcy immunostaining was previously reported in the stria vascularis of *Cx30*$^{-/-}$ null mice (25), also associated to reduced *Bhmt* expression, both data pointing towards BHMT as the key target for the regulation of cochlear Hcy levels. Again, these results suggest several mechanisms to explain cochlear dysfunction. First, homocysteinylation,

a post-translational modification leading to inactivation and aggregation of proteins with the consequent impairment of their function (53). Second, high Hcy levels, an independent risk factor for cardiovascular disease, as a determinant for atherosclerosis in the inner ear as suggested by several epidemiological reports (15-17). Third, the role Hcy, an agonist of N-methyl-D-aspartate receptors, in the overexcitation associated with hearing impairment (54, 55).

Oxidative stress is a condition associated with rapid ageing and which correlates with HL caused by noise or other noxious stimuli (44). Moreover, oxidative stress alters the function of several enzymes of Hcy metabolism (20, 41, 56, 57). Hence, impairment of Hcy metabolism in FD mice could rely on the effects of high levels of reactive oxygen and nitrogen species. Elimination of these damaging species is a key event to maintain the cell function (58-60), and requires the collective activities of a number of enzymes and redox buffers. The existence of oxidative stress in FD cochleae was revealed by: i) increased p22phox and MnSOD protein levels; ii) decreased expression of *Cat*, *Gpx4 and Gss*; iii) increased 3-NT levels in the stria vascularis and the spiral ganglion; and iv) increased GSH and GSSG levels. These results suggest increased ROS signaling involving the NOX complex (60), which may in turn cause the high level of apoptotic cells detected in the FD cochleae.

NOX are expressed in the rat cochlea and regulated by noxious stimuli such as noise (61). During oxidative stress, NOX3 and NOX4 protein levels remain unchanged, being NADPH oxidase activator subunits, such as p22phox, the main proteins involved in stress response (62). Parallel to NOX activation, the increase in MnSOD suggests an effort to eliminate the highly reactive superoxide ion, producing peroxide with lower reactivity. MnSOD is a marker of neuroprotection, which is triggered as a compensatory mechanism against stress (63). Interestingly, *Sod1*$^{-/-}$ null mice are deaf (64). However, the decrease in *Cat* expression in FD mice suggests a putative impairment in peroxide elimination through this reaction, an effect that could be larger if we consider the Hcy inhibition of the enzyme previously reported (65). Compensatory peroxide catabolism can be obtained through GPX, mainly GPX1, leading to increased GSSG production (66). GPX1 is able to use either GSH or the γ-glutamylcysteine produced in the first step of GSH synthesis (66), a fact that can overcome the small reduction detected in *Gss* expression in FD mice. Additionally, expression and enzyme levels may not correlate, given the complex regulation of glutathione synthesis that involves among others the antioxidant response elements in the gene promoters, post-translational modifications

and feedback inhibition by GSH (67). Therefore, a combination of γ-glutamylcysteine accumulation, increased GSH synthesis by stabilization of GCLC protein and/or augmented association to GCLM (lowering its K_m for glutamate and raising the K_i for GSH), together with elevated GSSG synthesis through GPX and imbalanced recycling through GSR, may explain conservation of a normal cochlear GSH/GSSG ratio in folate deficiency. The existence of a profound redox imbalance in the cochleae of FD mice was further confirmed by the detection of elevated 3-NT immunostaining. This metabolite is a product of peroxinitrite action, whose levels have been found augmented during oxidative stress in the aging ear (43).

Oxidative stress is also known to alter methionine and folate cycles at different levels. Several enzymes of these pathways are susceptible to this condition given their need for cofactors and metals (20, 41, 57). Therefore, a reduction in folate levels together with the cochlear oxidative stress detected not only remodels expression and protein levels, but is expected to modify enzyme activities, subcellular distribution and oligomerization as occurs in several experimental settings (56, 68-70). In this line, the increased p22phox levels in FD cochleae are expected to produce NOX activation, and hence lead to elevated $NADP^+$ concentrations. This metabolite is known to favor trimerization of methionine adenosyltransferase II reducing its affinity for methionine (57), an effect that in turn would guarantee the S-adenosylmethionine synthesis needed, among others, for epigenetic remodeling during nutritional stress. This effect may not be essential for FD mice receiving diets that supply enough methionine and cysteine for synthesizing the methyl donor and glutathione. However, it may derive from an effort to correct the altered methylation index resulting from the decreased cochlear AHCY levels that, in turn, would lead to increased S-adenosylhomocysteine concentrations and inhibition of transmethylations. An additional effect of impaired cochlear Hcy metabolism, precisely lower BHMT levels, is betaine accumulation. This increase in osmolyte concentrations might be beneficial to maintain the function of the thin cochlear basal epithelia of FD mice.

Altogether our results confirm that the ingestion of low levels of folic acid induces severe impairment of cochlear Hcy metabolism, together with a profound oxidative misbalance, ultimately leading to hearing loss. The positive correlation between hyperhomocysteinemia and hearing loss in folate deficiency also suggests the potential of the former as a prognostic value. In addition, targeting Hcy metabolism by

nutritional interventions could be a novel pathway to achieve therapeutic protection against hearing loss.

REFERENCES

1. Roth, T. N., Hanebuth, D., and Probst, R. (2011) Prevalence of age-related hearing loss in Europe: a review. *Eur. Arch. Otorhinolaryngol.* **268**, 1101-1107
2. Li-Korotky, H. S. (2012) Age-related hearing loss: quality of care for quality of life. *Gerontologist* **52**, 265-271
3. Dror, A. A., and Avraham, K. B. (2009) Hearing Loss: Mechanisms Revealed by Genetics and Cell Biology. *Annu. Rev. Genet.* **43**, 411-437
4. Liu, X. Z., and Yan, D. (2007) Ageing and hearing loss. *J. Pathol.* **211**, 188-197
5. Ohlemiller, K. K. (2006) Contributions of mouse models to understanding of age- and noise-related hearing loss. *Brain Res.* **1091**, 89-102
6. Tabuchi, K., Nishimura, B., Nakamagoe, M., Hayashi, K., Nakayama, M., and Hara, A. (2011) Ototoxicity: mechanisms of cochlear impairment and its prevention. *Curr. Med. Chem.* **18**, 4866-4871
7. Sliwinska-Kowalska, M., and Davis, A. (2012) Noise-induced hearing loss. *Noise & health* **14**, 274-280
8. Emmett, S. D., and West, K. P., Jr. (2014) Gestational vitamin A deficiency: A novel cause of sensorineural hearing loss in the developing world? *Med. Hypotheses* **82**, 6-10
9. Attias, J., Raveh, E., Aizer-Dannon, A., Bloch-Mimouni, A., and Fattal-Valevski, A. (2012) Auditory system dysfunction due to infantile thiamine deficiency: long-term auditory sequelae. *Audiol Neurootol* **17**, 309-320
10. Karli, R., Gul, A., and Ugur, B. (2013) Effect of vitamin B12 deficiency on otoacoustic emissions. *Acta Otorhinolaryngol. Ital.* **33**, 243-247
11. Houston, D. K., Johnson, M. A., Nozza, R. J., Gunter, E. W., Shea, K. J., Cutler, G. M., and Edmonds, J. T. (1999) Age-related hearing loss, vitamin B-12, and folate in elderly women. *Am. J. Clin. Nutr.* **69**, 564-571
12. Lasisi, A. O., Fehintola, F. A., and Yusuf, O. B. (2010) Age-related hearing loss, vitamin B12, and folate in the elderly. *Otolaryngol. Head Neck Surg.* **143**, 826-830
13. Cadoni, G., Agostino, S., Scipione, S., and Galli, J. (2004) Low serum folate levels: a risk factor for sudden sensorineural hearing loss? *Acta Otolaryngol* **124**, 608-611
14. Gok, U., Halifeoglu, I., Canatan, H., Yildiz, M., Gursu, M. F., and Gur, B. (2004) Comparative analysis of serum homocysteine, folic acid and Vitamin B12 levels in patients with noise-induced hearing loss. *Auris Nasus Larynx* **31**, 19-22
15. Johnsson, L. G., and Hawkins, J. E., Jr. (1972) Vascular changes in the human inner ear associated with aging. *Ann. Otol. Rhinol. Laryngol.* **81**, 364-376
16. Makishima, K. (1978) Arteriolar sclerosis as a cause of presbycusis. *Otolaryngology* **86**, ORL322-326
17. Rosen, S., and Olin, P. (1965) Hearing loss and coronary heart disease. *Bull. N Y Acad. Med.* **41**, 1052-1068
18. Jacques, P. F., Selhub, J., Bostom, A. G., Wilson, P. W., and Rosenberg, I. H. (1999) The effect of folic acid fortification on plasma folate and total homocysteine concentrations. *N Engl. J. Med.* **340**, 1449-1454
19. Durga, J., Verhoef, P., Anteunis, L. J., Schouten, E., and Kok, F. J. (2007) Effects of folic acid supplementation on hearing in older adults: a randomized, controlled trial. *Ann. Intern. Med.* **146**, 1-9

20. Pajares, M. A., and Perez-Sala, D. (2006) Betaine homocysteine S-methyltransferase: just a regulator of homocysteine metabolism? *Cell. Mol. Life Sci.* **63**, 2792-2803
21. Fusconi, M., Chistolini, A., de Virgilio, A., Greco, A., Massaro, F., Turchetta, R., Benincasa, A. T., Tombolini, M., and de Vincentiis, M. (2012) Sudden sensorineural hearing loss: a vascular cause? Analysis of prothrombotic risk factors in head and neck. *Int. J. Audiol.* **51**, 800-805
22. Uchida, Y., Sugiura, S., Ando, F., Nakashima, T., and Shimokata, H. (2011) Hearing impairment risk and interaction of folate metabolism related gene polymorphisms in an aging study. *BMC Med. Genet.* **12**, 35
23. Durga, J., Anteunis, L. J., Schouten, E. G., Bots, M. L., Kok, F. J., and Verhoef, P. (2006) Association of folate with hearing is dependent on the 5,10-methylenetetrahdyrofolate reductase 677C-->T mutation. *Neurobiol. Aging* **27**, 482-489
24. Kundu, S., Munjal, C., Tyagi, N., Sen, U., Tyagi, A. C., and Tyagi, S. C. (2012) Folic acid improves inner ear vascularization in hyperhomocysteinemic mice. *Hear. Res.* **284**, 42-51
25. Cohen-Salmon, M., Regnault, B., Cayet, N., Caille, D., Demuth, K., Hardelin, J. P., Janel, N., Meda, P., and Petit, C. (2007) Connexin30 deficiency causes instrastrial fluid-blood barrier disruption within the cochlear stria vascularis. *Proc. Natl. Acad. Sci. USA* **104**, 6229-6234
26. Maestro-de-las-Casas, C., Perez-Miguelsanz, J., Lopez-Gordillo, Y., Maldonado, E., Partearroyo, T., Varela-Moreiras, G., and Martinez-Alvarez, C. (2013) Maternal folic acid-deficient diet causes congenital malformations in the mouse eye. *Birth Defects Res.* **97**, 587-596
27. Maldonado, E., Murillo, J., Barrio, C., del Rio, A., Perez-Miguelsanz, J., Lopez-Gordillo, Y., Partearroyo, T., Paradas, I., Maestro, C., Martinez-Sanz, E., Varela-Moreiras, G., and Martinez-Alvarez, C. (2011) Occurrence of cleft-palate and alteration of Tgf-beta(3) expression and the mechanisms leading to palatal fusion in mice following dietary folic-acid deficiency. *Cells Tissues Organs* **194**, 406-420
28. Ison, J. R., Allen, P. D., and O'Neill, W. E. (2007) Age-related hearing loss in C57BL/6J mice has both frequency-specific and non-frequency-specific components that produce a hyperacusis-like exaggeration of the acoustic startle reflex. *J. Assoc. Res. Otolaryngol.* **8**, 539-550
29. Keithley, E. M., Canto, C., Zheng, Q. Y., Fischel-Ghodsian, N., and Johnson, K. R. (2004) Age-related hearing loss and the ahl locus in mice. *Hear. Res.* **188**, 21-28
30. Teng, Y. W., Mehedint, M. G., Garrow, T. A., and Zeisel, S. H. (2011) Deletion of murine betaine-homocysteine S-methyltransferase in mice perturbs choline and 1-carbon metabolism, resulting in fatty liver and hepatocellular carcinoma. *J. Biol. Chem.* **286**, 36258-36267
31. Cediel, R., Riquelme, R., Contreras, J., Diaz, A., and Varela-Nieto, I. (2006) Sensorineural hearing loss in insulin-like growth factor I-null mice: a new model of human deafness. *Eur. J. Neurosci.* **23**, 587-590
32. Murillo-Cuesta, S., Camarero, G., Gonzalez-Rodriguez, A., De La Rosa, L. R., Burks, D. J., Avendano, C., Valverde, A. M., and Varela-Nieto, I. (2012) Insulin receptor substrate 2 (IRS2)-deficient mice show sensorineural hearing loss that is delayed by concomitant protein tyrosine phosphatase 1B (PTP1B) loss of function. *Mol. Med.* **18**, 260-269

33. Rodriguez-de la Rosa, L., Lopez-Herradon, A., Portal-Nunez, S., Murillo-Cuesta, S., Lozano, D., Cediel, R., Varela-Nieto, I., and Esbrit, P. (2014) Treatment with N- and C-terminal peptides of parathyroid hormone-related protein partly compensate the skeletal abnormalities in IGF-I deficient mice. *PloS One* **9**, e87536
34. Sanchez-Calderon, H., Rodriguez-de la Rosa, L., Milo, M., Pichel, J. G., Holley, M., and Varela-Nieto, I. (2010) RNA microarray analysis in prenatal mouse cochlea reveals novel IGF-I target genes: implication of MEF2 and FOXM1 transcription factors. *PloS One* **5**, e8699
35. Camarero, G., Avendano, C., Fernandez-Moreno, C., Villar, A., Contreras, J., de Pablo, F., Pichel, J. G., and Varela-Nieto, I. (2001) Delayed inner ear maturation and neuronal loss in postnatal Igf-1-deficient mice. *J. Neurosci.* **21**, 7630-7641
36. Aburto, M. R., Magarinos, M., Leon, Y., Varela-Nieto, I., and Sanchez-Calderon, H. (2012) AKT signaling mediates IGF-I survival actions on otic neural progenitors. *PloS One* **7**, e30790
37. Horne, D. W., and Patterson, D. (1988) Lactobacillus casei microbiological assay of folic acid derivatives in 96-well microtiter plates. *Clin. Chem.* **34**, 2357-2359
38. Tamura, T. (1990) Microbiological assays of folates. In *Folic acid metabolism in health and disease* (Piccairo, M. F., Stokstad, R., and Gregory, J. F., eds) pp. 121-137, Wiley-Liss, Inc., New York, USA
39. Rahman, I., Kode, A., and Biswas, S. K. (2006) Assay for quantitative determination of glutathione and glutathione disulfide levels using enzymatic recycling method. *Nat. Protoc.* **1**, 3159-3165
40. Rodriguez-de la Rosa, L., Fernandez-Sanchez, L., Germain, F., Murillo-Cuesta, S., Varela-Nieto, I., de la Villa, P., and Cuenca, N. (2012) Age-related functional and structural retinal modifications in the Igf1-/- null mouse. *Neurobiol. Dis.* **46**, 476-485
41. Delgado, M., Perez-Miguelsanz, J., Garrido, F., Rodriguez-Tarduchy, G., Perez-Sala, D., and Pajares, M. A. (2008) Early effects of copper accumulation on methionine metabolism. *Cell. Mol. Life Sci.* **65**, 2080-2090
42. Pfaffl, M. W. (2001) A new mathematical model for relative quantification in real-time RT-PCR. *Nucleic Acids Res.* **29**, e45
43. Jiang, H., Talaska, A. E., Schacht, J., and Sha, S. H. (2007) Oxidative imbalance in the aging inner ear. *Neurobiol. Aging* **28**, 1605-1612
44. Kujawa, S. G., and Liberman, M. C. (2009) Adding insult to injury: cochlear nerve degeneration after "temporary" noise-induced hearing loss. *J. Neurosci.* **29**, 14077-14085
45. Feng, H., Yin, S. H., and Tang, A. Z. (2011) Blocking caspase-3-dependent pathway preserves hair cells from salicylate-induced apoptosis in the guinea pig cochlea. *Mol. Cell. Biochem.* **353**, 291-303
46. Tropitzsch, A., Arnold, H., Bassiouni, M., Muller, A., Eckhard, A., Muller, M., and Lowenheim, H. (2014) Assessing cisplatin-induced ototoxicity and otoprotection in whole organ culture of the mouse inner ear in simulated microgravity. *Toxicol. Lett.* **227**, 203-212
47. Pajares, M. A., and Markham, G. D. (2011) Methionine adenosyltransferase (s-adenosylmethionine synthetase). *Adv. Enzymol. Relat. Areas Mol. Biol.* **78**, 449-521

48. Vlajkovic, S. M., Guo, C. X., Dharmawardana, N., Wong, A. C., Boison, D., Housley, G. D., and Thorne, P. R. (2010) Role of adenosine kinase in cochlear development and response to noise. *J. Neurosci. Res*. **88**, 2598-2609
49. Hornbeck, P. V., Kornhauser, J. M., Tkachev, S., Zhang, B., Skrzypek, E., Murray, B., Latham, V., and Sullivan, M. (2012) PhosphoSitePlus: a comprehensive resource for investigating the structure and function of experimentally determined post-translational modifications in man and mouse. *Nucl. Acids Res.* **40**, 261-270
50. Yamada, K., Kawata, T., Wada, M., Isshiki, T., Onoda, J., Kawanishi, T., Kunou, A., Tadokoro, T., Tobimatsu, T., Maekawa, A., and Toraya, T. (2000) Extremely low activity of methionine synthase in vitamin B-12-deficient rats may be related to effects on coenzyme stabilization rather than to changes in coenzyme induction. *J. Nutr.* **130**, 1894-1900
51. Vlajkovic, S. M., Guo, C. X., Telang, R., Wong, A. C., Paramananthasivam, V., Boison, D., Housley, G. D., and Thorne, P. R. (2011) Adenosine kinase inhibition in the cochlea delays the onset of age-related hearing loss. *Exp. Gerontol.* **46**, 905-914
52. Li, X., Mao, X. B., Hei, R. Y., Zhang, Z. B., Wen, L. T., Zhang, P. Z., Qiu, J. H., and Qiao, L. (2011) Protective role of hydrogen sulfide against noise-induced cochlear damage: a chronic intracochlear infusion model. *PloS One* **6**, e26728
53. Jakubowski, H., and Glowacki, R. (2011) Chemical biology of homocysteine thiolactone and related metabolites. *Adv. Clin. Chem.* **55**, 81-103
54. Lipton, S. A., Kim, W. K., Choi, Y. B., Kumar, S., D'Emilia, D. M., Rayudu, P. V., Arnelle, D. R., and Stamler, J. S. (1997) Neurotoxicity associated with dual actions of homocysteine at the N-methyl-D-aspartate receptor. *Proc. Natl. Acad. Sci. USA* **94**, 5923-5928
55. Puel, J. L., Ladrech, S., Chabert, R., Pujol, R., and Eybalin, M. (1991) Electrophysiological evidence for the presence of NMDA receptors in the guinea pig cochlea. *Hear. Res.* **51**, 255-264
56. Pajares, M. A., Alvarez, L., and Perez-Sala, D. (2013) How are mammalian methionine adenosyltransferases regulated in the liver? A focus on redox stress. *FEBS Lett.* **587**, 1711-1716
57. Gonzalez, B., Garrido, F., Ortega, R., Martinez-Julvez, M., Revilla-Guarinos, A., Perez-Pertejo, Y., Velazquez-Campoy, A., Sanz-Aparicio, J., and Pajares, M. A. (2012) NADP+ binding to the regulatory subunit of methionine adenosyltransferase II increases intersubunit binding affinity in the hetero-trimer. *PloS One* **7**, e50329
58. Radi, R. (2013) Peroxynitrite, a stealthy biological oxidant. *J. Biol. Chem.* **288**, 26464-26472
59. Banerjee, R. (2012) Redox outside the box: linking extracellular redox remodeling with intracellular redox metabolism. *J. Biol. Chem.* **287**, 4397-4402
60. Lambeth, J. D., and Neish, A. S. (2014) Nox enzymes and new thinking on reactive oxygen: a double-edged sword revisited. *Annu. Rev. Pathol.* **24**, 119-145
61. Vlajkovic, S. M., Lin, S. C., Wong, A. C., Wackrow, B., and Thorne, P. R. (2013) Noise-induced changes in expression levels of NADPH oxidases in the cochlea. *Hear. Res.* **304**, 145-152

62. Kundu, S., Tyagi, N., Sen, U., and Tyagi, S. C. (2009) Matrix imbalance by inducing expression of metalloproteinase and oxidative stress in cochlea of hyperhomocysteinemic mice. *Mol. Cell. Biochem.* **332**, 215-224
63. Sanchez-Alcazar, J. A., Schneider, E., Hernandez-Munoz, I., Ruiz-Cabello, J., Siles-Rivas, E., de la Torre, P., Bornstein, B., Brea, G., Arenas, J., Garesse, R., Solis-Herruzo, J. A., Knox, A. J., and Navas, P. (2003) Reactive oxygen species mediate the down-regulation of mitochondrial transcripts and proteins by tumour necrosis factor-alpha in L929 cells. *Biochem. J.* **370**, 609-619
64. Keithley, E. M., Canto, C., Zheng, Q. Y., Wang, X., Fischel-Ghodsian, N., and Johnson, K. R. (2005) Cu/Zn superoxide dismutase and age-related hearing loss. *Hear. Res.* **209**, 76-85
65. Milton, N. G. N. (2008) Homocysteine Inhibits Hydrogen Peroxide Breakdown by Catalase. *Open Enzym. Inhib. J.* **1**, 34-41
66. Quintana-Cabrera, R., Fernandez-Fernandez, S., Bobo-Jimenez, V., Escobar, J., Sastre, J., Almeida, A., and Bolanos, J. P. (2012) gamma-Glutamylcysteine detoxifies reactive oxygen species by acting as glutathione peroxidase-1 cofactor. *Nat. Commun.* **3**, 718
67. Lu, S. C. (2013) Glutathione synthesis. *Biochim. Biophys. Acta* **1830**, 3143-3153
68. Lu, S. C., and Mato, J. M. (2012) S-adenosylmethionine in liver health, injury, and cancer. *Physiol. Rev.* **92**, 1515-1542
69. Delgado, M., Garrido, F., Perez-Miguelsanz, J., Pacheco, M., Partearroyo, T., Perez-Sala, D., and Pajares, M. A. (2014) Acute Liver Injury Induces Nucleocytoplasmic Redistribution of Hepatic Methionine Metabolism Enzymes. *Antioxid. Redox Signal.* **20**, 2541-2554
70. Mosharov, E., Cranford, M. R., and Banerjee, R. (2000) The quantitatively important relationship between homocysteine metabolism and glutathione synthesis by the transsulfuration pathway and its regulation by redox changes. *Biochemistry* **39**, 13005-13011
71. Gonzalez, B., Campillo, N., Garrido, F., Gasset, M., Sanz-Aparicio, J., and Pajares, M. A. (2003) Active-site-mutagenesis study of rat liver betaine-homocysteine S-methyltransferase. *Biochem. J.* **370**, 945-952

ACKNOWLEDGMENTS

RMV is supported by a fellowship of the JAE-CSIC predoctoral program. The authors wish to thank Estela Maldonado from Complutense University of Madrid and the Genomics and Non-invasive Neurofunctional Evaluation facilities (IIBM, CSIC-UAM) for the technical support provided. We would also like to warmly thank our colleagues at the Neurobiology of Hearing group for sharing unpublished data and helpful discussions. This work was supported by grants of the Ministerio de Ciencia e Innovación (BFU2008-00666 and BFU2009-08977 to MAP; SAF2011-24391 to IVN; PS09/01762 to CMA), the European Union (FP7-AFHELO and TARGEAR to IVN), US National Institutes of Health (DK056350 to SHZ) and Puleva BioFoods (to IVN, GVM and MAP). The funders had no role in study design, data collection and analysis, decision to publish, or preparation of the manuscript.

The authors declare no conflict of interest.

TABLE LEGENDS

Table 1. Antibodies used in this study. The table lists the antibodies used in this work indicating the dilutions used for the different techniques.
*Abbreviations used are as follows: IC-P, immunohistochemistry-paraffin; IHF, immunohistofluorescence; WB, western blotting.
** tertiary extrAvidin® peroxidase-conjugated antibody (1:300 v/v; Sigma-Aldrich) was needed in this case.

Table 2. Primer sequences used for Real-Time RT-PCR experiments. Appropriate primers for genes in the methionine cycle and related pathways were designed using the Program Primer Express 3.0 and the mouse gene sequences available in the data bank with references: NC_000068.6 (*Ada*); NC_000080.5 (*Adk*); NW_000085.1 (*Bhmt*); NC_000079.5 (*Bhmt2*); NC_000083 (*Cbs*); NT_039207 (*Ahcy*); NC_000079 (*Mtr*); NC_000080.5 (*Mat1a*); NC_000072.5 (*Mat2a*); NC_000077.5 (*Mat2b*); NC_000072.6 (*Rn18s*). Base numbers indicate the location of the primer sequences in the corresponding mRNA; primers for *Cbs* and *Adk* were designed in regions common to the two splicing forms reported. The concentrations of the primers used for SYBR Green detection are shown in the right column.

FIGURE LEGENDS

Figure 1. Pathways involved in homocysteine metabolism and systemic metabolite levels. (A) Scheme of homocysteine metabolism and related pathways. Metabolites appear in white boxes and the enzymes listed include: adenosine deaminase (ADA); adenosine kinase (ADK); AdoHcy hydrolase (AHCY); betaine homocysteine methyltransferases (BHMTs); AdoMet-dependent methyltransferases (MTs); methionine adenosyltransferases (MATs); vitamin B6-dependent cystathionine β-synthase (CBS); and vitamin B12-dependent methionine synthase (MTR). (B) Serum and plasma metabolite levels from all the animals in both normal (NF) and folate-deficient (FD) groups are shown. Serum folic acid [50.85 ± 22.03 (n=10) vs. 7.46 ± 3.88 μg/l (n=11)], plasma Hcy [5.05 ± 2.45 (n=33) vs. 14.70 ± 3.19 μM (n=69)] and plasma vitamin B6 levels [40.00 ± 15.71 (n=11) vs. 43.71 ± 8.74 μg/l (n=18)] were measured as specified in the Materials and Methods section. The figure shows the mean ± SEM for each group and differences were considered significant when $p \leq 0.05$; (***) $p < 0.0001$.

Figure 2. Folate deficient mice show early signs of hearing loss. The auditory response was analyzed in mice of normal (NF) and folate-deficient (FD) groups. (A) Scheme of the auditory pathway. (B) Representative ABR recordings in response to click stimuli of NF (showing normal hearing) and FD mice (showing profound hearing loss). (C) ABR thresholds in response to click and tone burst stimuli in NF (○) and FD (●) mice, after 8 weeks of diet (n=21 for each group). (D) Latency-intensity function for wave I of NF and FD mice showing a delay in the appearance of the wave. Data are shown as the mean ± SEM, (**) $p<0.01$; (***) $p<0.001$.

Figure 3. Folate-deficient mice showed altered cochlear morphology and apoptotic cells. Cochlear morphology from normal (NF) and folate-deficient mice (FD) was studied by histochemistry and immunohistofluorescence. (A) Representative micrographs show basal and middle turn details of the organ of Corti in sections of NF (a-e; n=6) and FD mice (f-j; n=9). Phalloidin (Phal) staining of the organ of Corti appears in panels d, e, i and j. Stars denote the flat epithelium of the organ of Corti in panel g. Stars indicate the absence of hair cells. (B) Representative images and quantification of cell death by TUNEL assay of the organ of Corti per ROI from the middle turn of both groups. (C) Percentage of TUNEL-positive cells/ROI in the stria vascularis from the FD mice in comparison with the NF (n=6 mice studied per experimental group). IHC, inner hair cells; OHC, outer hair cells; SV, scala vestibulae; ST, scala tympani; SM, scala media. Scale bars: 500 µm (a,f); 50 µm (d,e,i,j) and 25 µm (b,c,g,h).

Figure 4. Folate-deficient mice showed altered cochlear cytoarchitecture. Sections of cochleae from mice on normal (A-H; n=6) or folate-deficient (J-Q; n=9) diets were stained with Masson's Trichrome, H&E or used for immunofluorescence. Basal and middle turn details of the ligament (Spl), cochlear ganglion (CG) and stria vascularis (StV) are shown. Immunohistochemistry results of the cochlear ganglion neurons labeled with myelin protein zero are shown at higher magnification in the insets to panels D, E, M and N. Details of the stria vascularis immunolabeled with Kir4.1 (Kir4.1) are included as insets to panels G, H, P and Q. Arrows indicate the absence of cells (J, M). Scale bars: 25 µm (A-H, J-Q and insets to G, H, P, Q); 10 µm (insets to D, E, M, N). Panel C depicts a scheme of the cochlea where basal and middle turns are indicated by squares. The intensity of the signals (0 to 256 grey scale) was quantified for normal (NF; n=4) and folate-deficient (FD; n=6) samples and the results are shown as the mean ± SEM in F, I, L, O, R histograms. (**) $p<0.01$ and (***) $p<0.001$.

Figure 5. Cochlear homocysteine metabolism in control mice. Samples of cochleae from mice receiving a normal folate diet were used to characterize Hcy metabolism and related reactions. (A) Total cochlear RNA was used to analyze expression levels of the genes of interest by real-time RT-PCR. Data were normalized using the *Rn18s* gene as reference and the results were referred to *Mat1a* levels set arbitrarily to 10 for graphical purposes (n=6). (B-D) Total cochlear proteins from wild type and *Bhmt*$^{-/-}$ null mice (200 μg), as well as cytosols from hepatoma H35 cells (3 μg), were used to verify the specificity of the bands detected on western blots. Membranes were incubated with: (B) rabbit anti-BHMT (71) and mouse anti-tubulin; (C) preimmune serum; and (D) goat anti-AHCY. The size of the prestained markers is indicated on the left side of the blots.

Figure 6. Folate deficiency alters expression of genes involved in Hcy metabolism. Total cochlear RNA of mice on normal (NF, n=11) or folate deficient (FD, n=12) diets was used to analyze expression levels of the genes of interest by real-time RT-PCR using the *Rn18s* gene as reference. The results are shown as the mean ± SEM of determinations made in triplicate for each animal sample. Statistical analysis by Student´s t-test was carried out using GraphPad Prism and data considered significant when $p \leq 0.05$ (*).

Figure 7. Effects of folate deficiency on cochlear protein levels of enzymes involved in homocysteine metabolism. Total cochlear protein (200 μg/lane) of animals in normal (NF; n=11) and folate-deficient (FD; n=20) diets were analyzed by western blot using the following antibodies: (A) anti-AHCY; (B) anti-CBS; (C) anti-BHMT; (D) anti-MTR; (E) anti-ADK; and (F) anti-ADA. Representative immunoblots for each antibody are shown, together with quantifications (mean ± SEM) carried out with ImageJ software, normalized using tubulin as the loading control. For graphical purposes, the mean of the NF group ratio was considered 100% in each case. Statistical analysis was carried out using Student's t-test and differences were consider significant when $p \leq 0.05$ (*). (G) Representative image of anti-homocysteine western blot on NF and FD mice and its densitometric analysis. Mean data of the NF group are presented as 100% for graphical purposes, being the ratios 3.92 ± 0.80 (NF; n=4) and 6.28 ± 1.06 (FD; n=5).

Figure 8. Folate deficient mice showed oxidative imbalance in the cochlea. Cochleae from mice on normal (NF) and folate-deficient (FD) diets were used to

evaluate several oxidative stress markers. (A) Schematic representation of the role of the oxidative stress markers analyzed in this work. (B) Representative immunoblots for NADPH oxidase (NOX4; n=3 NF and n=4 FD), MnSOD (n=6 NF and n=9 FD) and p22phox (n=5 NF and n=9 FD). The histograms show the mean ± SEM of densitometric scanning results after normalization using β-actin levels. (C) Expression levels of *Cat*, *Gpx1*, *GPx4*, *Gsr*, *Gclc* and *Gss* evaluated by real-time RT-PCR using *Rplp0* as reference. (D) Evaluation of cochlear oxidized (GSSG) and reduced (GSH) glutathione levels (n=6 mice per group). (E) Representative images of 3-nitrotyrosine (3-NT) levels detected by immunohistochemistry in the stria vascularis (StV; a,b) and cochlear ganglion (SG; c,d) of NF (a,c; n=3) and FD (b,d; n=6) mice. (e) Quantification of the 3-NT signal is shown in the histograms as the mean ± SEM. Statistical evaluation of the data was performed by Student's t-test: (*) $p<0,05$; (**) $p<0,01$: (***) $p<0.001$.

Table 1.

Primary antibody	Source	Dilution (v/v)	Secondary antibody	Source	Dilution (v/v)	Technique*
Chicken anti-Myelin P0	Novus Biologicals (NB100-1607)	1:100	IgG Rabbit anti-chicken biotin-conjugated	Acris Antibodies (R1300B)	1:300	IC-P**
Rabbit anti-3-nitrotyrosine	Millipore (AB5411)	1:200	IgG goat anti-rabbit biotin-conjugated	Chemicon-Millipore (AQ132B)	1:300	IC-P**
Rabbit anti-Kir4.1	Chemicon (AB5818)	1:200	IgG donkey anti-rabbit Alexa Fluor 488	Molecular Probes (A21206)	1:400	IHF
Mouse anti-β-actin	Sigma (A5441)	1:5000	IgG sheep anti-mouse HRP conjugated	GE Healthcare (NA931)	1:5000	WB
Mouse anti-α-Tubulin	Sigma (T9026)	1:2500	IgG sheep anti-mouse HRP conjugated	GE Healthcare (NA931)	1:20000	WB
Mouse anti-CBS	Abnova (H00000875-A01)	1:2500	IgG sheep anti-mouse HRP conjugated	GE Healthcare (NA931)	1:20000	WB
Rabbit anti-BHMT	González et al. [1]	1:5000	IgG goat anti-rabbit HRP conjugated	Bio-Rad (170-6515)	1:5000	WB
Rabbit anti-ADK	Abcam (ab88903)	1:500	IgG goat anti-rabbit HRP conjugated	Bio-Rad (170-6515)	1:5000	WB
Rabbit anti-Hcy	Chemicon-Millipore (AB5512)	1:1000	IgG goat anti-rabbit HRP conjugated	Bio-Rad (170-6515)	1:3000	WB
Rabbit anti-p22phox	Santa Cruz (sc-20781)	1:500	IgG goat anti-rabbit HRP conjugated	Bio-Rad (170-6515)	1:3000	WB
Rabbit anti-MnSOD	Upstate Millipore (06-984)	1:2500	IgG goat anti-rabbit HRP conjugated	Bio-Rad (170-6515)	1:3000	WB
Goat anti-AHCY	Santa Cruz (sc-66759)	1:1000	IgG donkey anti-goat HRP conjugated	Santa-Cruz (sc-2020)	1:10000	WB
Goat anti-MTR	Abnova (PAB6022)	1:250	IgG donkey anti-goat HRP conjugated	Santa-Cruz (sc-2020)	1:10000	WB
Goat anti-ADA	Santa Cruz (sc-7451)	1:2500	IgG donkey anti-goat HRP conjugated	Santa-Cruz (sc-2020)	1:10000	WB
Goat anti-NOX4	Santa Cruz (sc-21860)	1:500	IgG donkey anti-goat HRP conjugated	Santa-Cruz (sc-2020)	1:3000	WB

Table 2.

Gene	Bases	Forward primer (5'-3')	Bases	Reverse primer (5'-3')	nM
Ada	641-663	GGGATGAGACCATTGAAGGAAGT	709-689	TCTTTACTGCGCCCTCATAGG	300
Adk	883-903	AGAGGCAGAGGACCGTGATCT	946-925	TCATTCTCTGCAGCCACTATGG	300
Bhmt	672-692	CAGAATTCCCCTTTGGATTGG	742-721	GGCCTCTCTGGCATATTTTTGA	300
Bhmt2	143-166	CTCCAGAAGCAGTGGTAGAACATC	217-198	CATCAGCTCCCGCTCTCAAG	300
Cbs	1274-1292	GCAGCGCTGTGTGGTCATC	1337-1312	GTCACTCAGGAACTTGGACATGTAGT	300
Ahcy	1531-1554	TCGAAGTGTCCAATGTTACAGACA	1592-1575	CTTGGCCGGCACTTTGAG	300
Mtr	2006-2026	CGCGATCAAGTTTGGTATGGA	2080-2057	TCCTTGTGGATAGCATCATACACA	300
Mat1a	1285-1307	GGTGTTATTGTCAGGGACTTGGA	1347-1329	GCCGTAGCACGCAGTCTTC	300
Mat2a	1057-1079	GGAGGGTTCTTGTTCAGGTCTCT	1123-1102	TGGAAAATGGAGATCGACAATG	300
Mat2b	134-153	GCTGGTGGAGGAGGAAGTGA	192-173	CAGTGGCACCGGTAATGAGA	300
Rn18s	1645-1666	CCAGTAAGTGCGGGTCATAAGC	1716-1737	CCGATTGGATGGTTTAGTGAGG	100

A

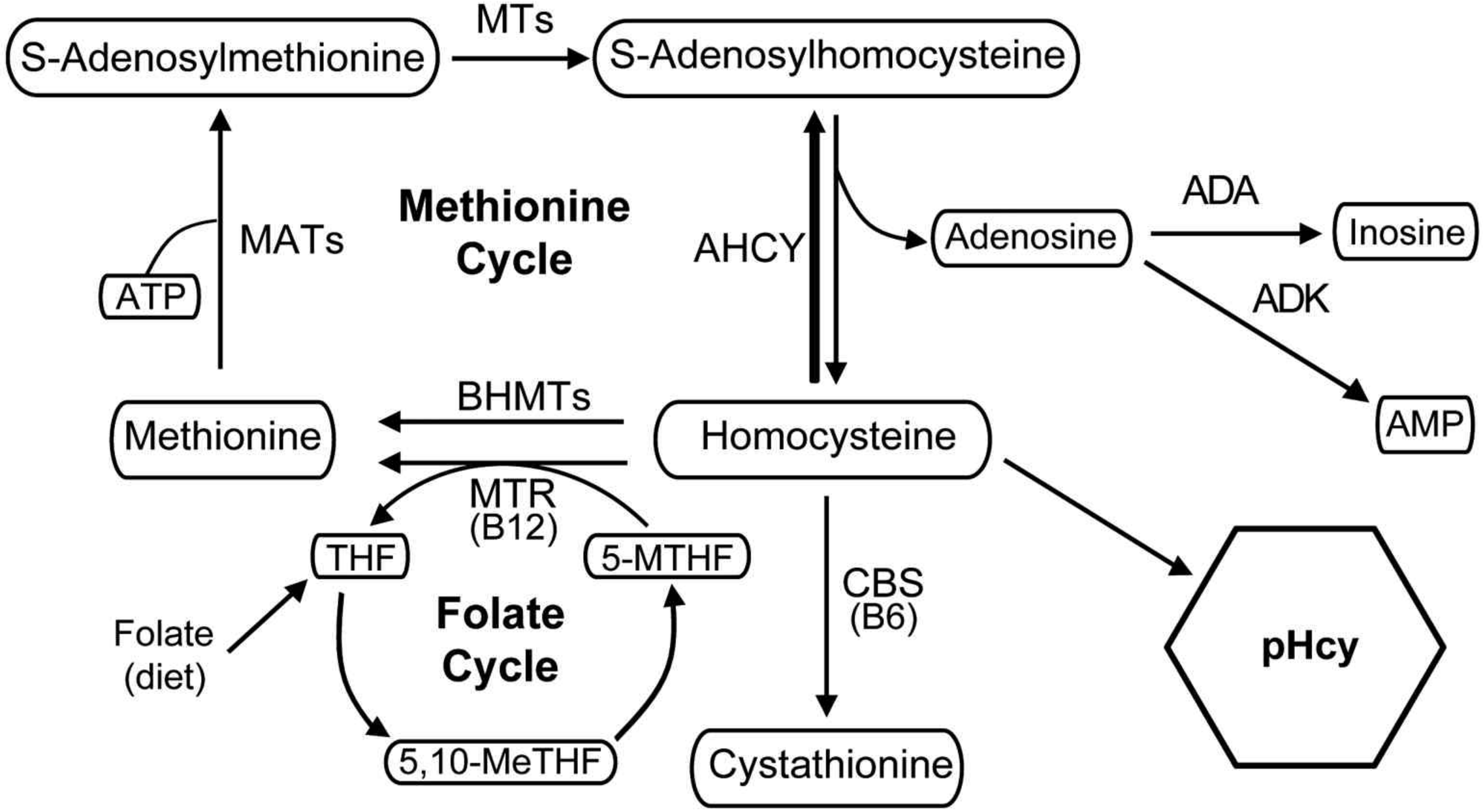
S-Adenosylmethionine
MTs
S-Adenosylhomocysteine
MATs
ATP
Methionine Cycle
AHCY
Adenosine
ADA
Inosine
ADK
AMP
BHMTs
Methionine
Homocysteine
MTR (B12)
THF
5-MTHF
Folate (diet)
Folate Cycle
CBS (B6)
pHcy
5,10-MeTHF
Cystathionine

B

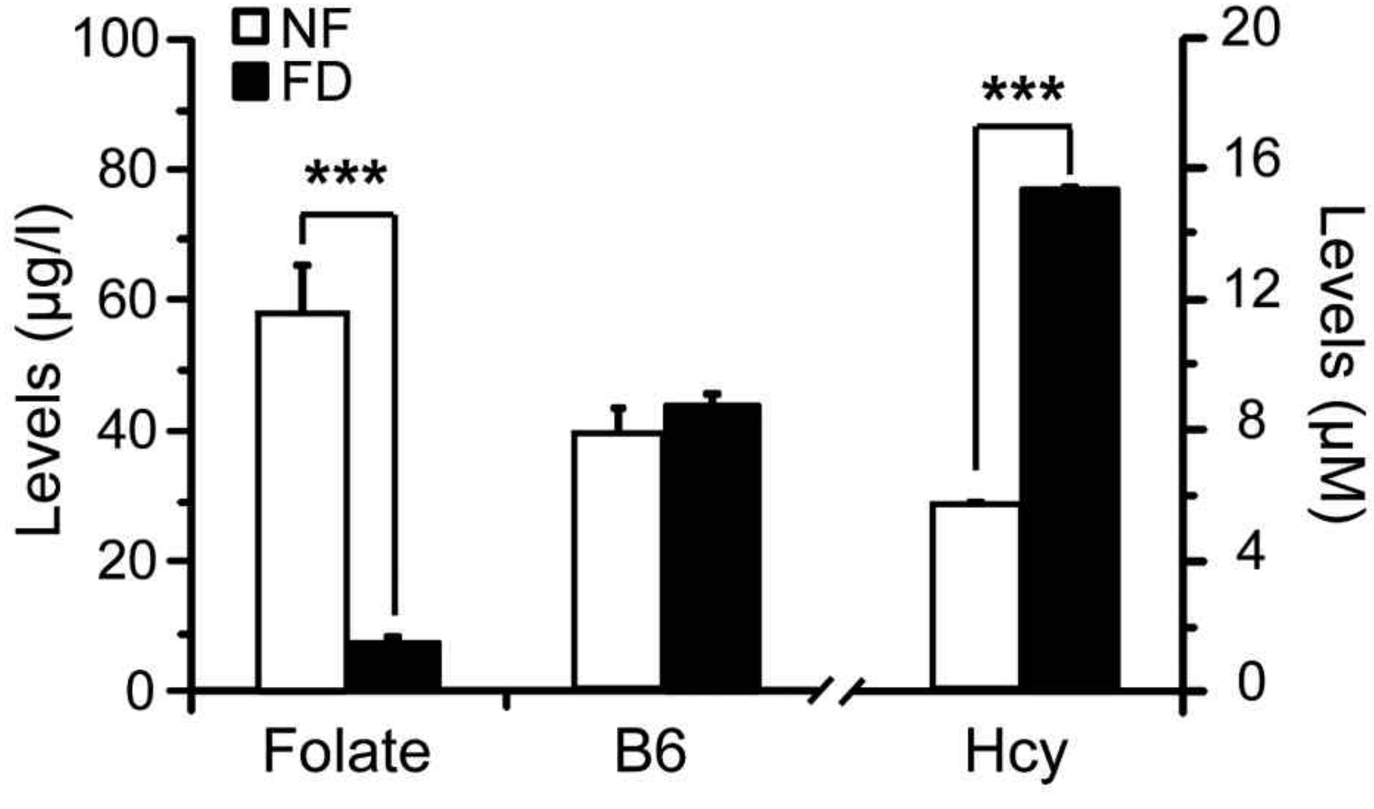
NF
FD
***
***
Levels (μg/l)
Levels (μM)
100
80
60
40
20
0
20
16
12
8
4
0
Folate
B6
Hcy

A

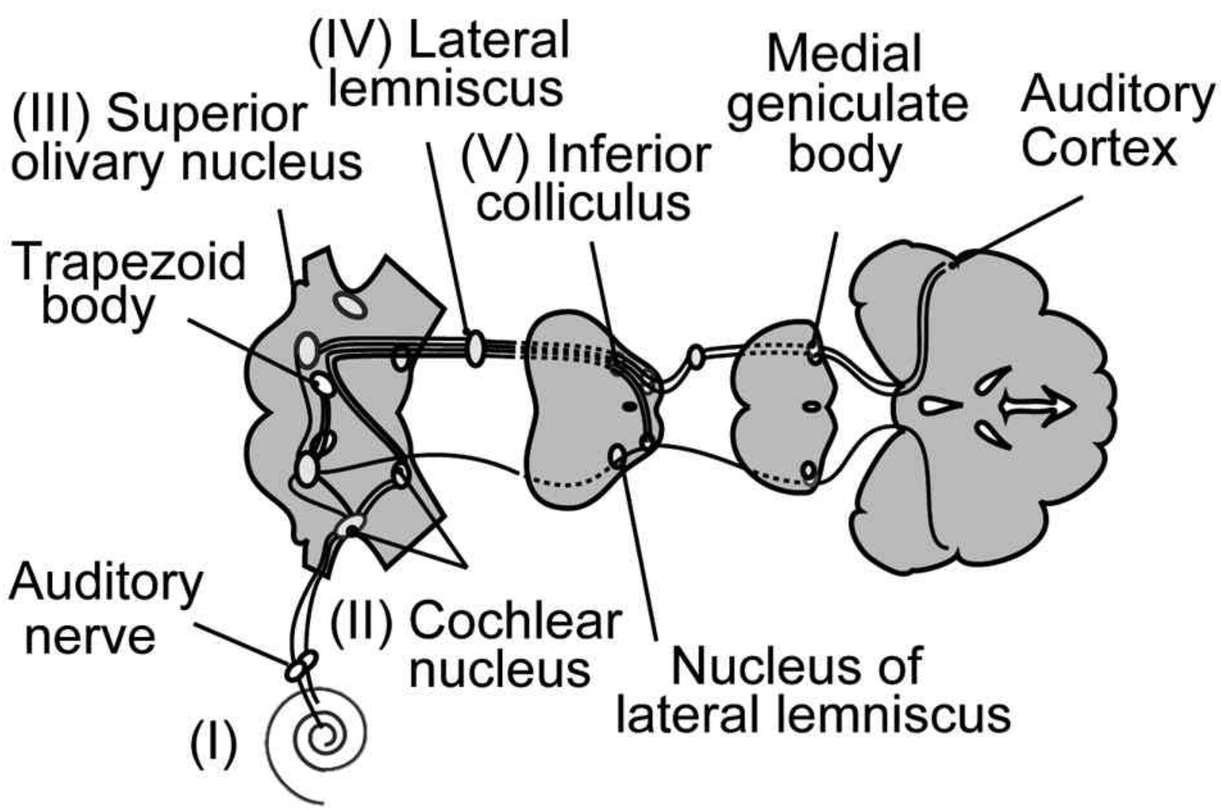
(IV) Lateral lemniscus
Medial geniculate body
Auditory Cortex
(III) Superior olivary nucleus
(V) Inferior colliculus
Trapezoid body
Auditory nerve
(II) Cochlear nucleus
Nucleus of lateral lemniscus
(I)

B

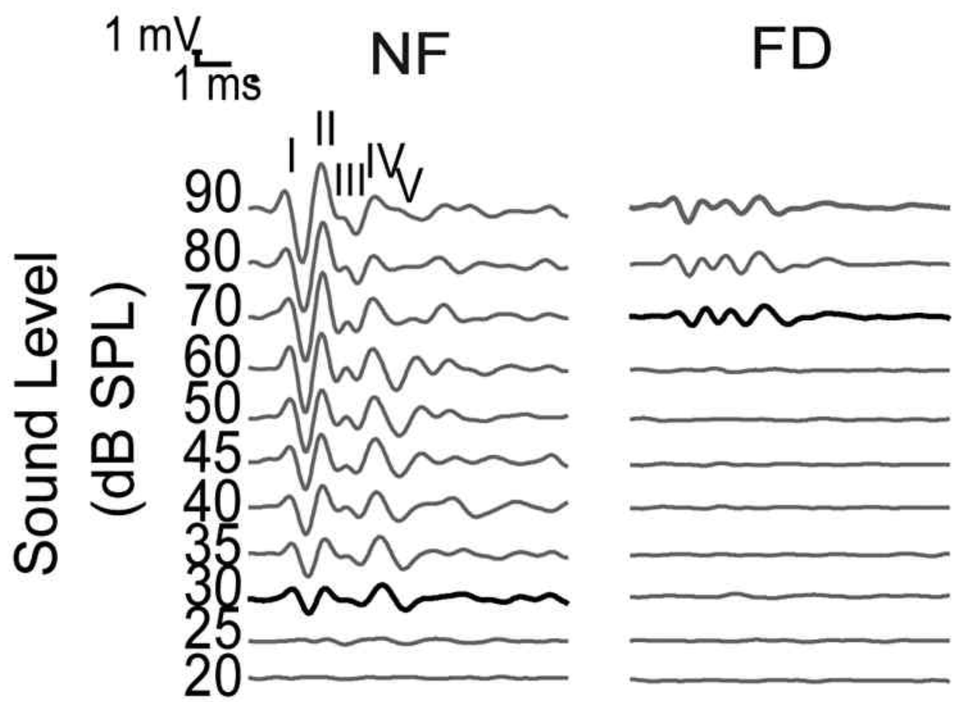
1 mV
1 ms
NF
FD
I
II
III
IV
V
Sound Level (dB SPL)
90
80
70
60
50
45
40
35
30
25
20

C

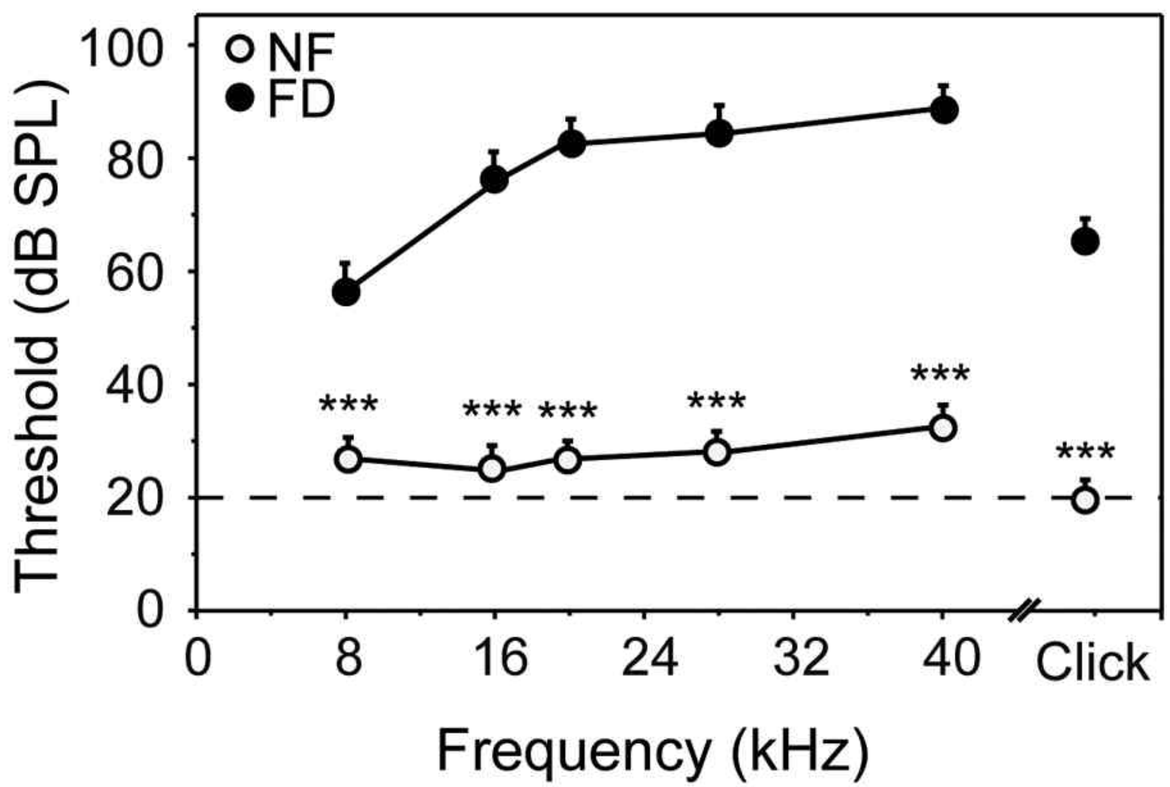
NF
FD
Threshold (dB SPL)
100
80
60
40
20
0
***
0
8
16
24
32
40
Click
Frequency (kHz)

D

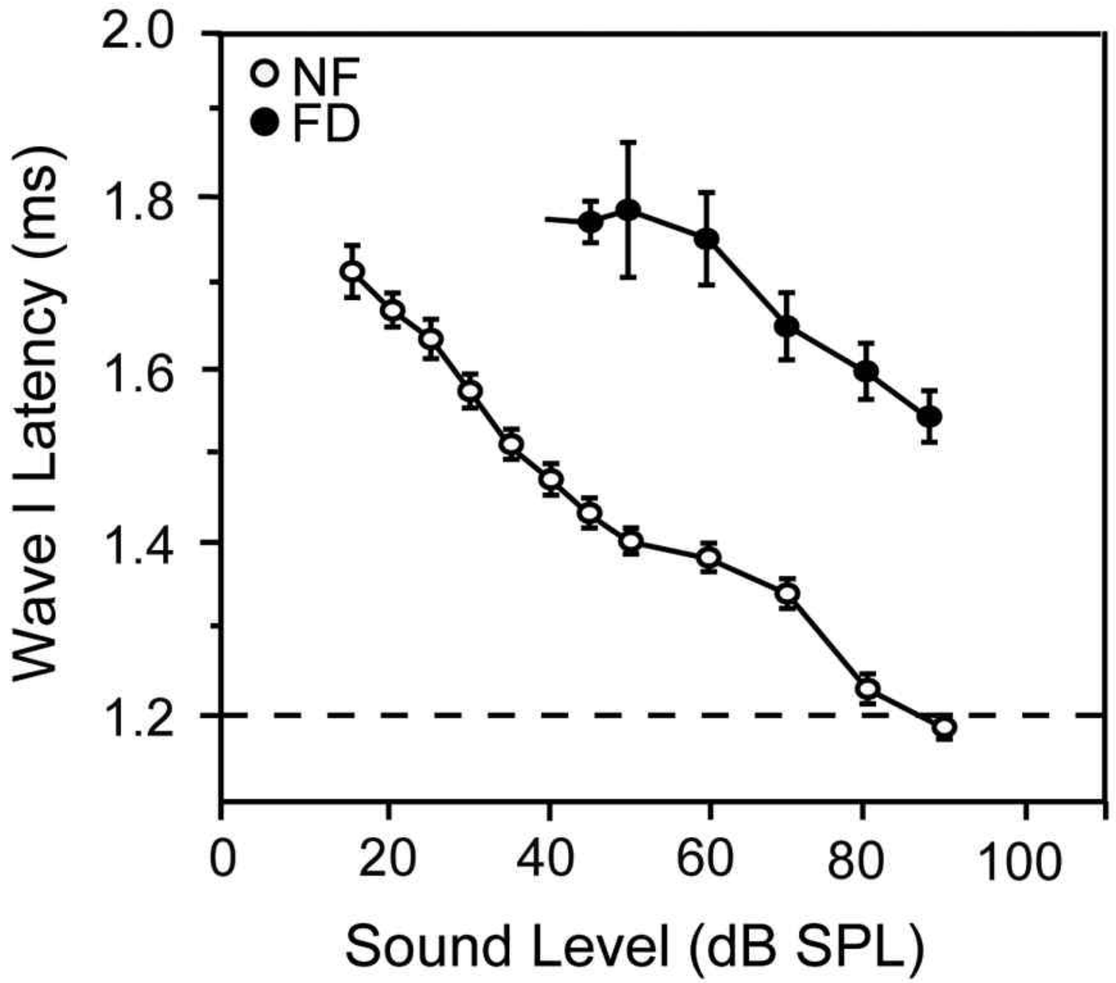
NF
FD
Wave I Latency (ms)
2.0
1.8
1.6
1.4
1.2
0
20
40
60
80
100
Sound Level (dB SPL)

Normal Folate

Folate Deficient

a

Apex

SV

SM

ST

Base

f

b

OHC IHC

Base

c

Middle

g

***

Base

h

Middle

d

Phal/DAPI

e

Phal/DAPI

i

***

Phal/DAPI

j

Phal/DAPI

B

NF

Middle

TUNEL

FD

Middle

TUNEL

TUNEL+ cells (%)

400

300

200

100

0

***

NF FD

C

NF

Middle

TUNEL

FD

Middle

TUNEL

TUNEL+ cells (%)

400

300

200

100

0

***

NF FD

Normal Folate

Folate Deficient

Spl

CG

StV

A Base

B Middle

C

Apex

Base

D

D´

E

E´

Myelin P0

F

CG staining intensity

200

150

100

50

0

**

NF FD

G

G´

H

H´

Kir4.1

I

Myeling P0 staining intensity

BASAL TURN

150

100

50

0

***

NF FD

J Base

K Middle

L

Myeling P0 staining intensity

MIDDLE TURN

150

100

50

0

NF FD

M

M´

N

N´

Myelin P0

O

Kir4.1 staining intensity

BASAL TURN

150

100

50

0

NF FD

P

P´

Q

Q´

Kir4.1

R

Kir4.1 staining intensity

MIDDLE TURN

150

100

50

0

NF FD

A

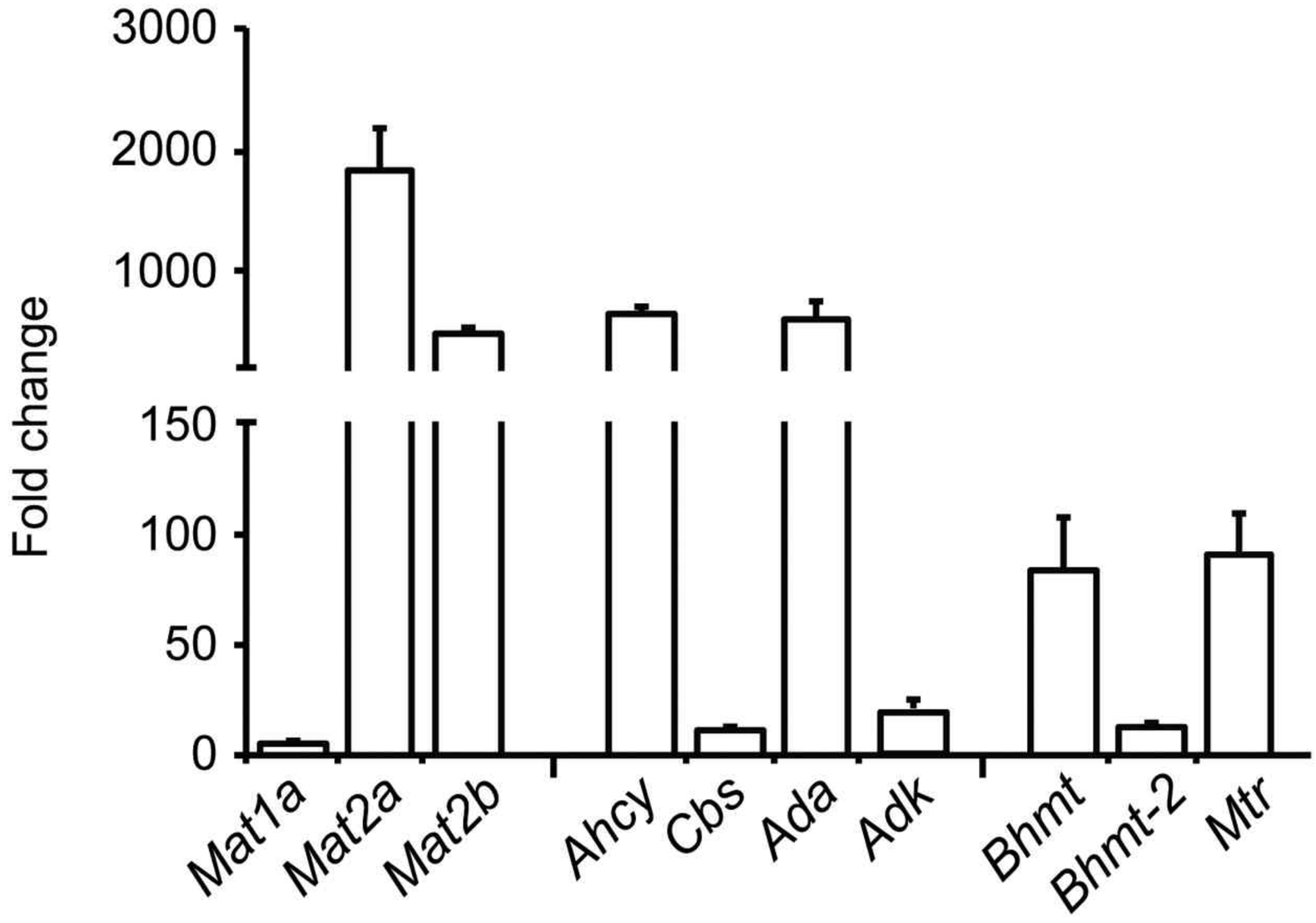
3000
2000
1000
150
100
50
0
Fold change
Mat1a
Mat2a
Mat2b
Ahcy
Cbs
Ada
Adk
Bhmt
Bhmt-2
Mtr

B

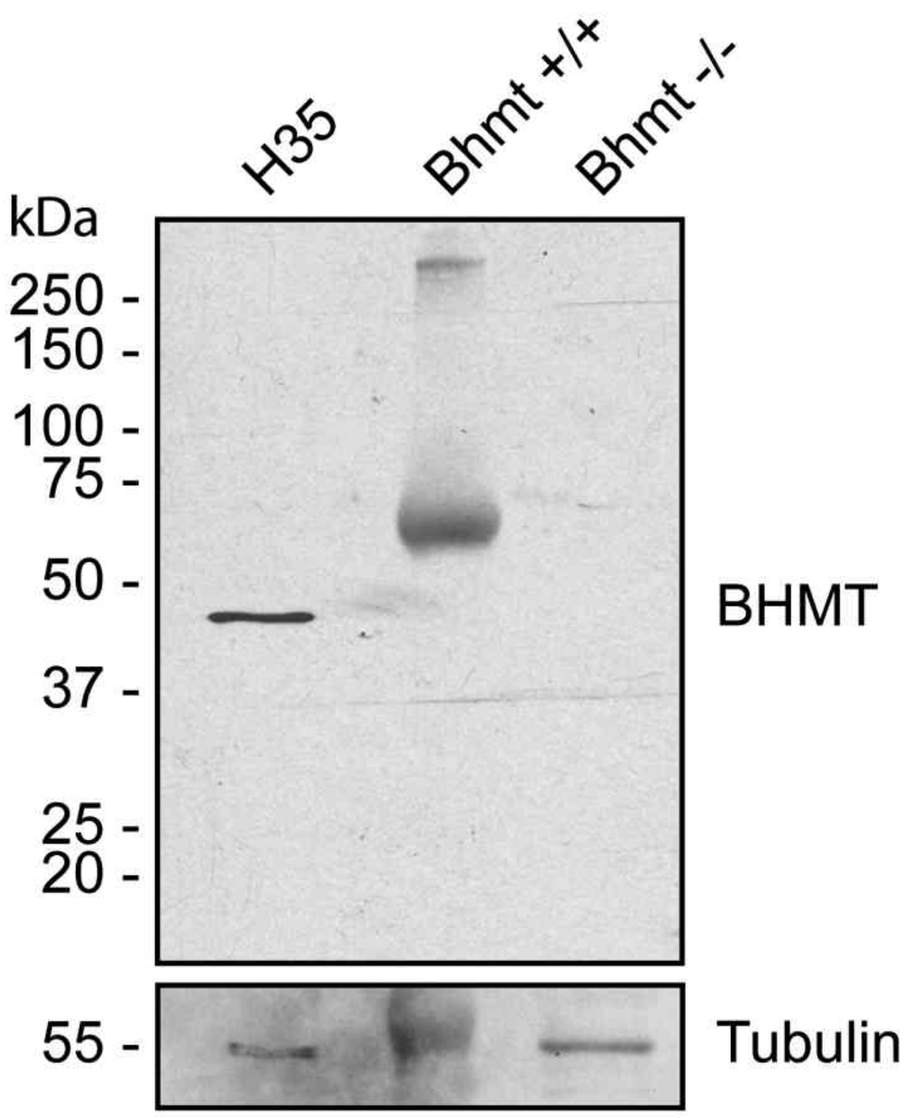
H35
Bhmt +/+
Bhmt -/-
kDa
250 -
150 -
100 -
75 -
50 -
37 -
25 -
20 -
BHMT
55 -
Tubulin

C

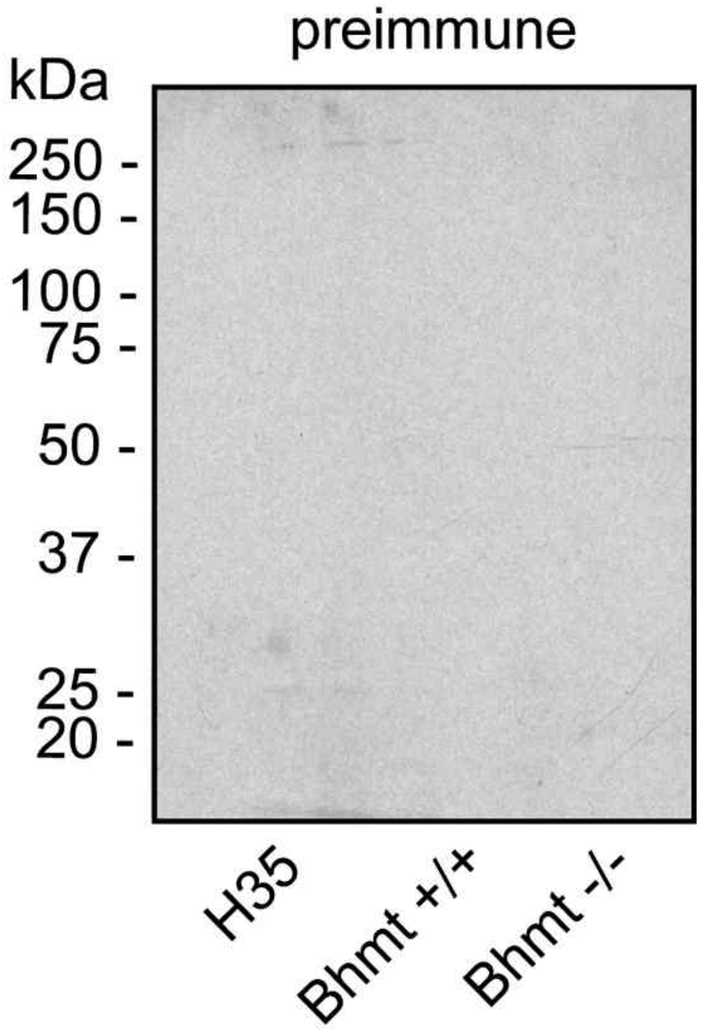
preimmune
kDa
250 -
150 -
100 -
75 -
50 -
37 -
25 -
20 -
H35
Bhmt +/+
Bhmt -/-

D

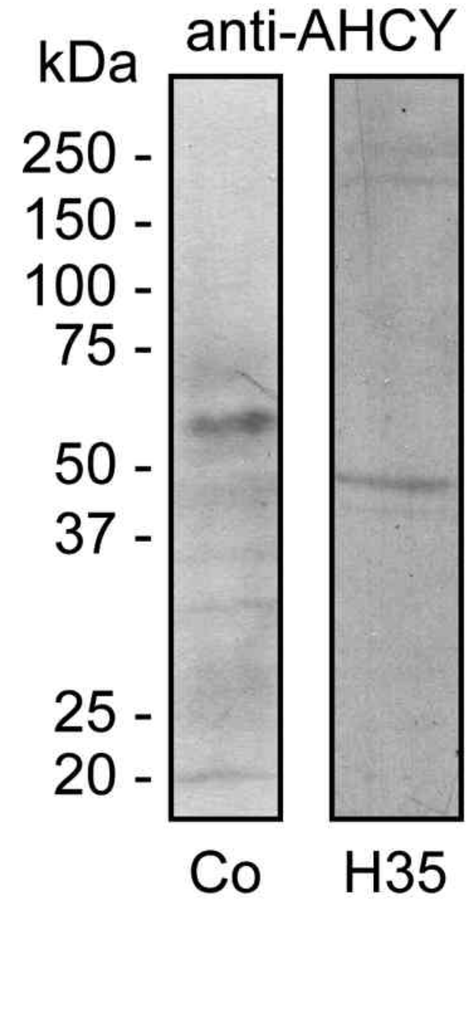
anti-AHCY
kDa
250 -
150 -
100 -
75 -
50 -
37 -
25 -
20 -
Co
H35

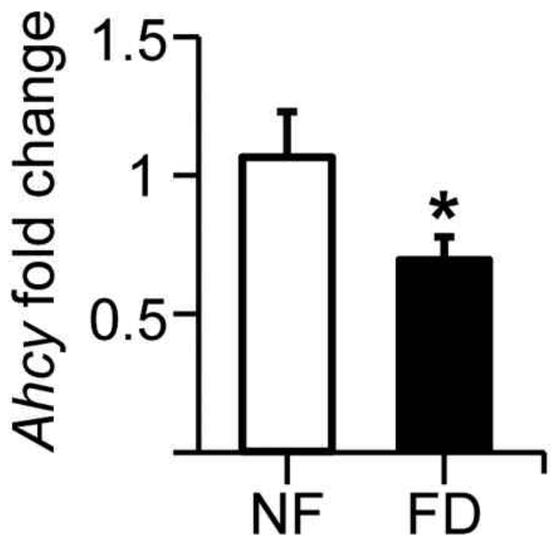
Ahcy fold change
1.5
1
0.5
*
NF
FD

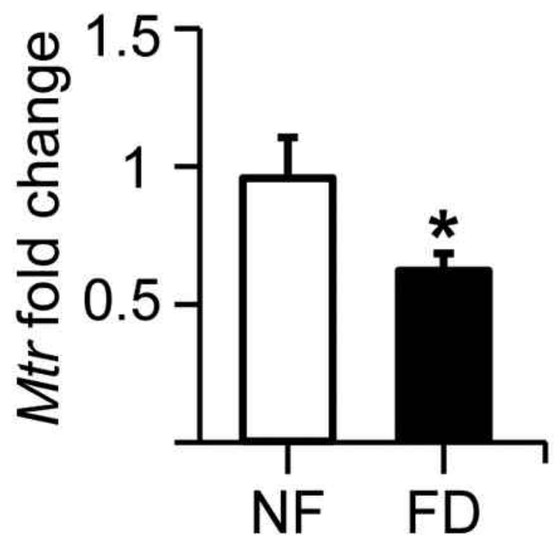
Mtr fold change
1.5
1
0.5
*
NF
FD

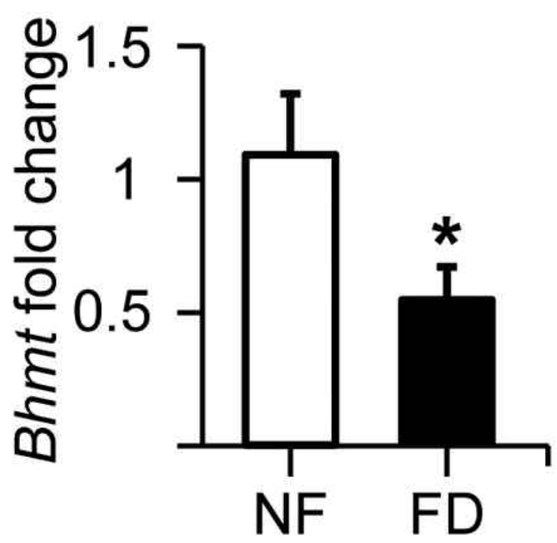
Bhmt fold change
1.5
1
0.5
*
NF
FD

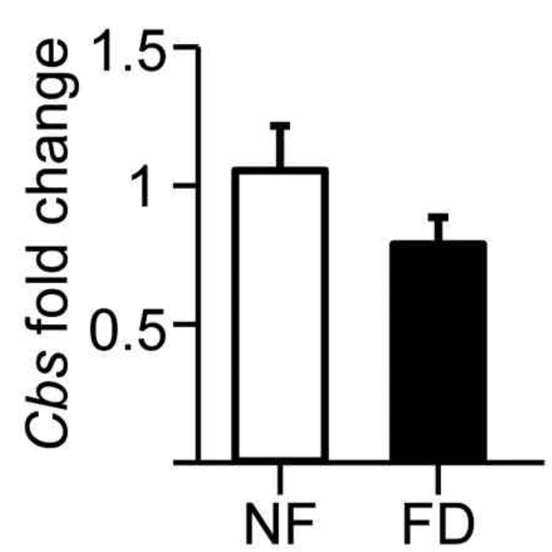
Cbs fold change
1.5
1
0.5
NF
FD

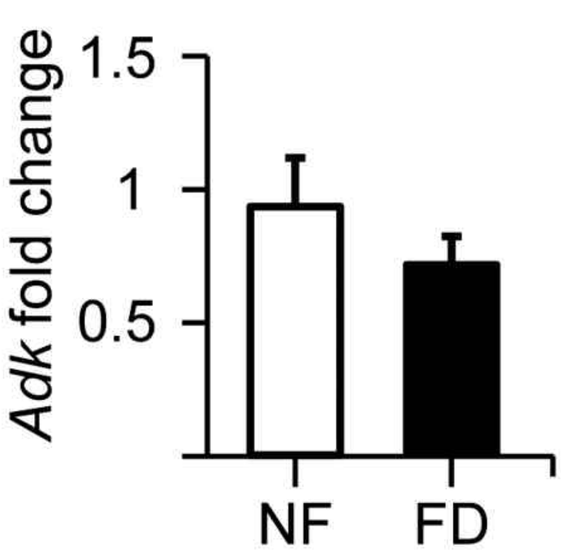
Adk fold change
1.5
1
0.5
NF
FD

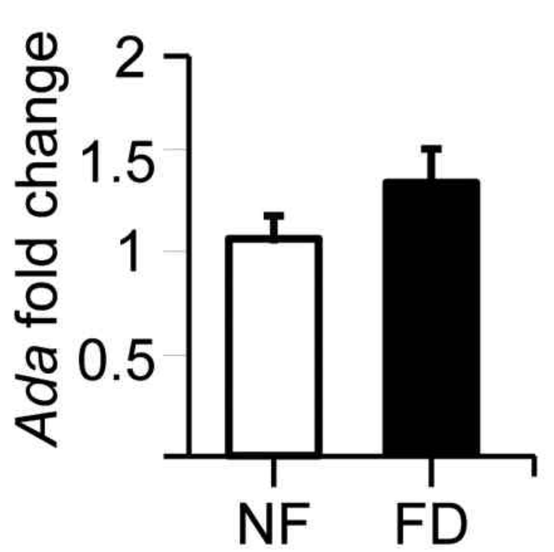
Ada fold change
2
1.5
1
0.5
NF
FD

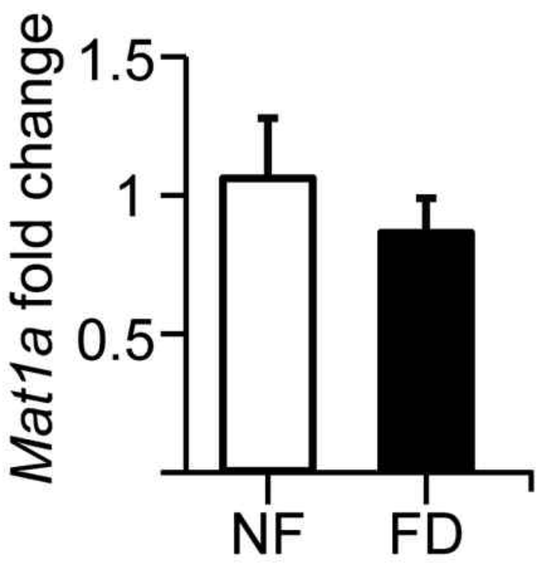
Mat1a fold change
1.5
1
0.5
NF
FD

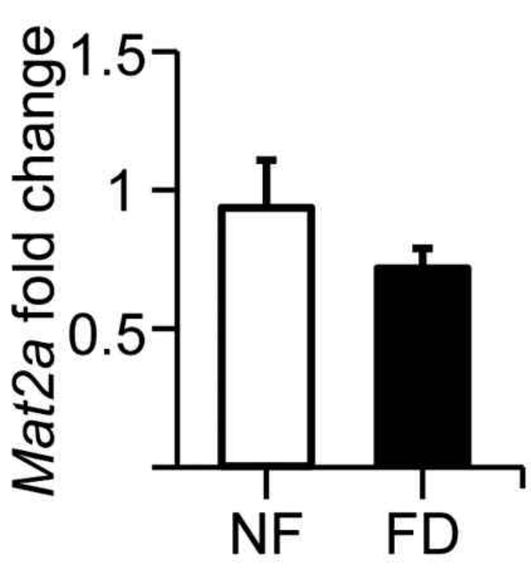
Mat2a fold change
1.5
1
0.5
NF
FD

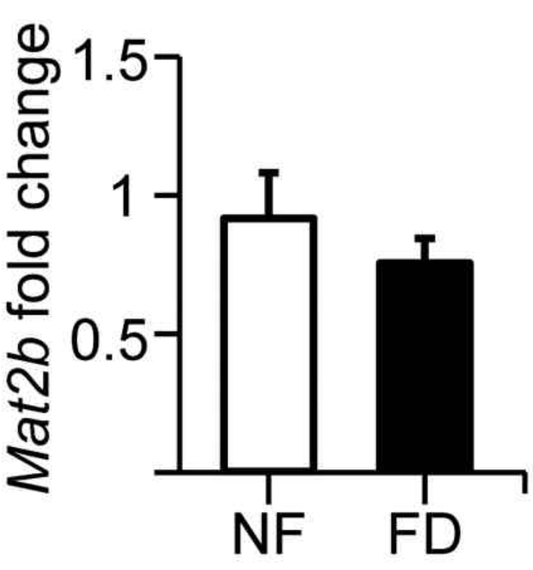
Mat2b fold change
1.5
1
0.5
NF
FD

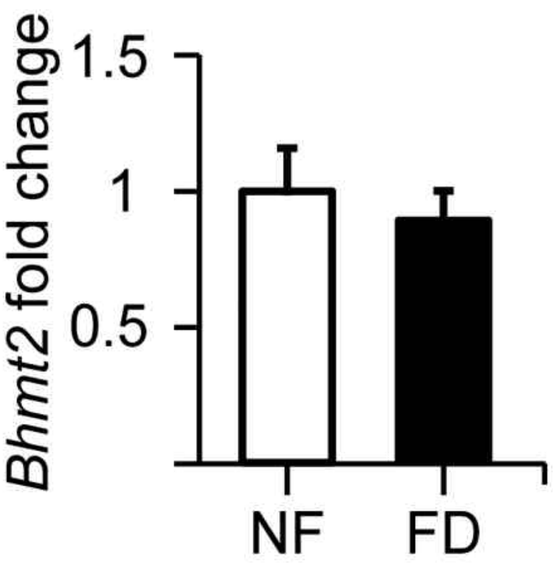
Bhmt2 fold change
1.5
1
0.5
NF
FD

A

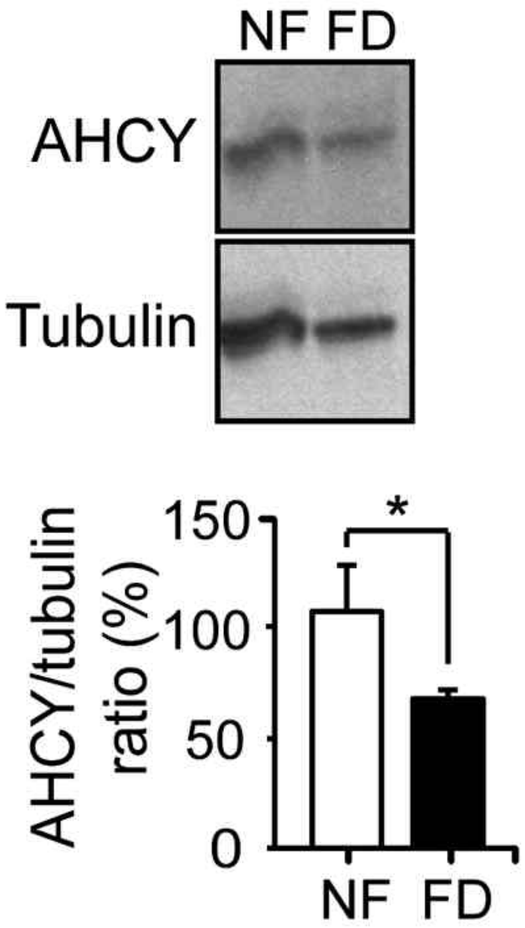
NF FD
AHCY
Tubulin
AHCY/tubulin ratio (%)
150
100
50
0
*
NF FD

B

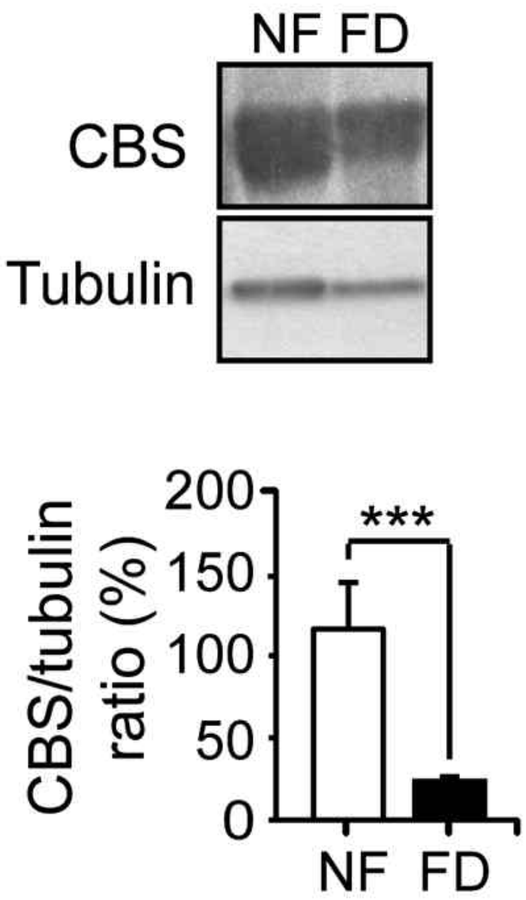
NF FD
CBS
Tubulin
CBS/tubulin ratio (%)
200
150
100
50
0
***
NF FD

C

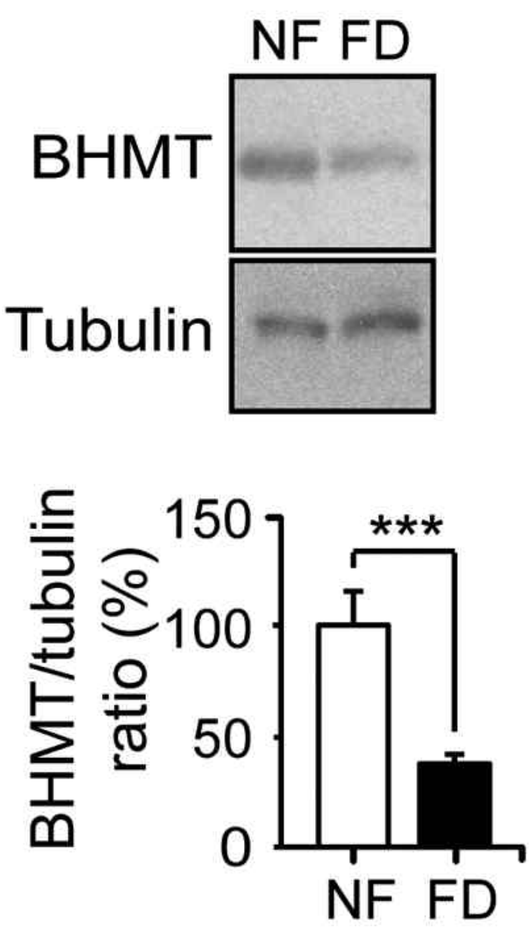
NF FD
BHMT
Tubulin
BHMT/tubulin ratio (%)
150
100
50
0
***
NF FD

D

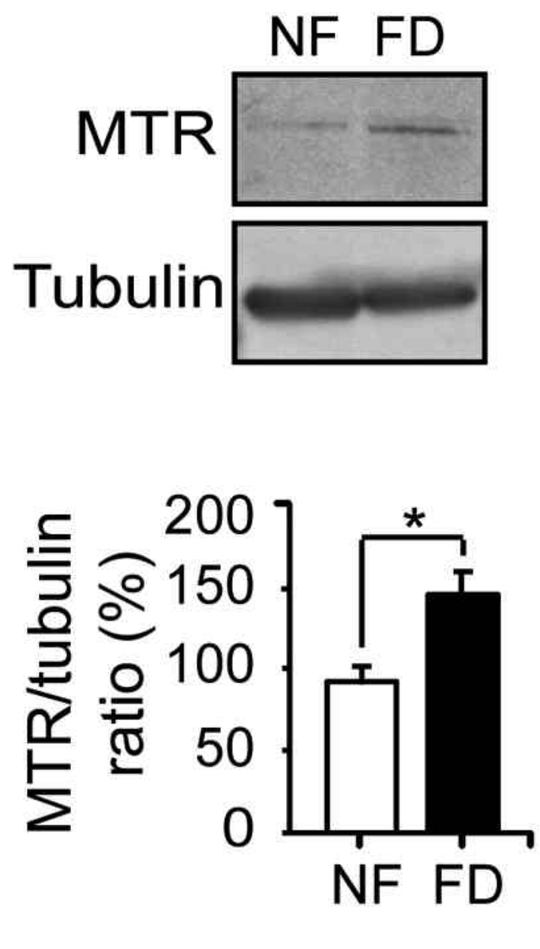
NF FD
MTR
Tubulin
MTR/tubulin ratio (%)
200
150
100
50
0
*
NF FD

E

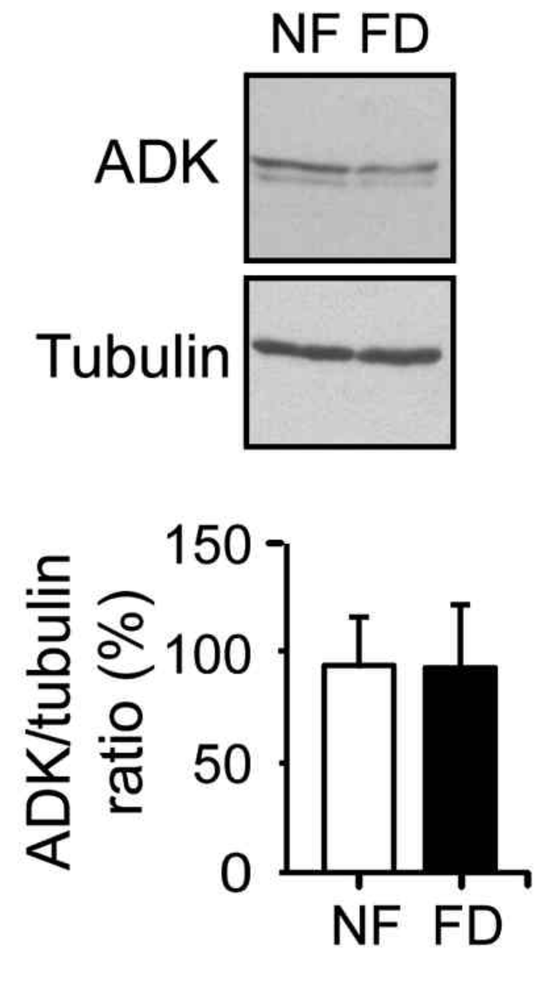
NF FD
ADK
Tubulin
ADK/tubulin ratio (%)
150
100
50
0
NF FD

F

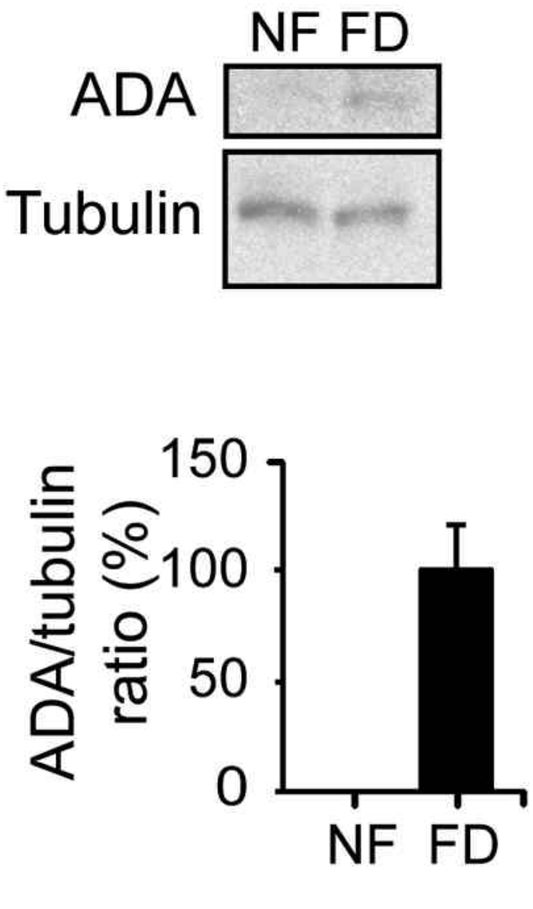
NF FD
ADA
Tubulin
ADA/tubulin ratio (%)
150
100
50
0
NF FD

J

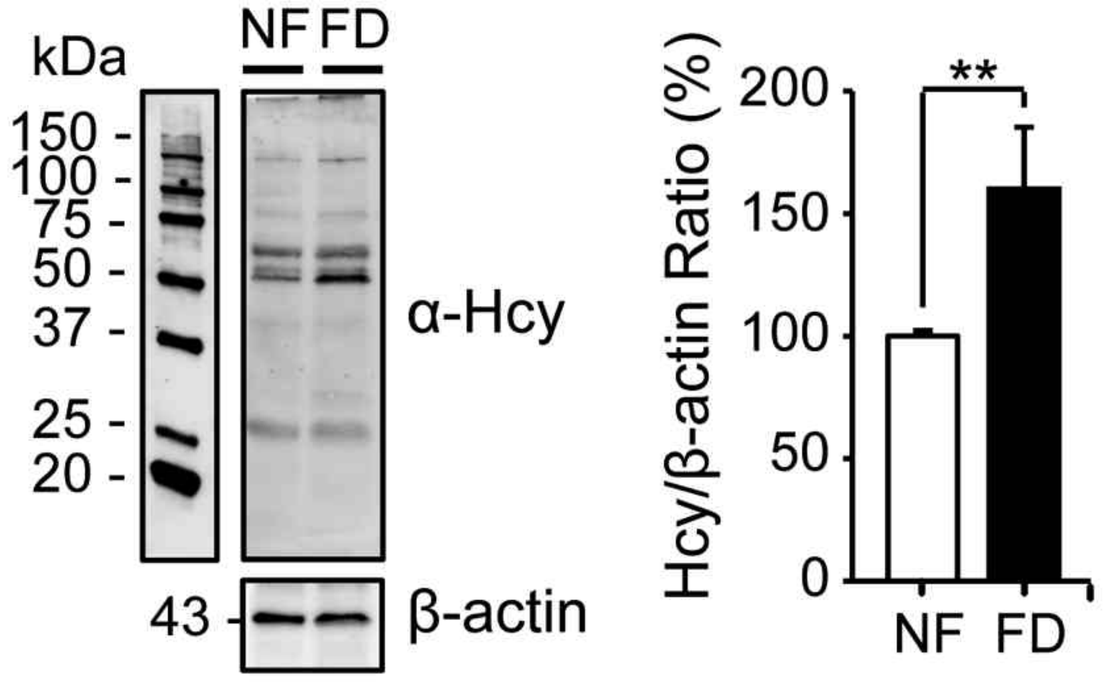
kDa
NF FD
150 -
100 -
75 -
50 -
37 -
25 -
20 -
α-Hcy
43 -
β-actin
Hcy/β-actin Ratio (%)
200
150
100
50
0
**
NF FD

A

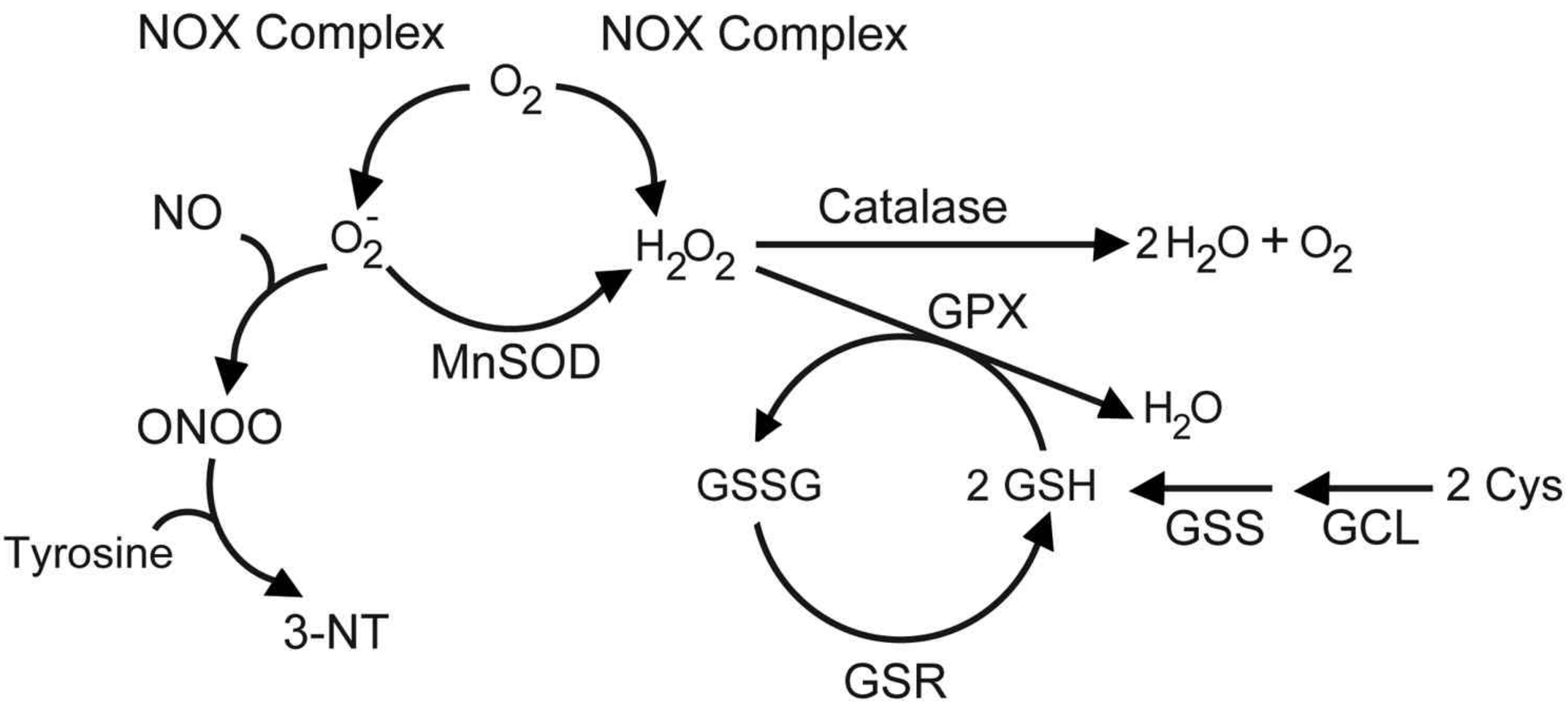
NOX Complex
NOX Complex
O_2
NO
O_2^-
H_2O_2
Catalase
$2H_2O + O_2$
GPX
MnSOD
H_2O
ONOO
GSSG
2 GSH
2 Cys
GSS
GCL
Tyrosine
3-NT
GSR

B

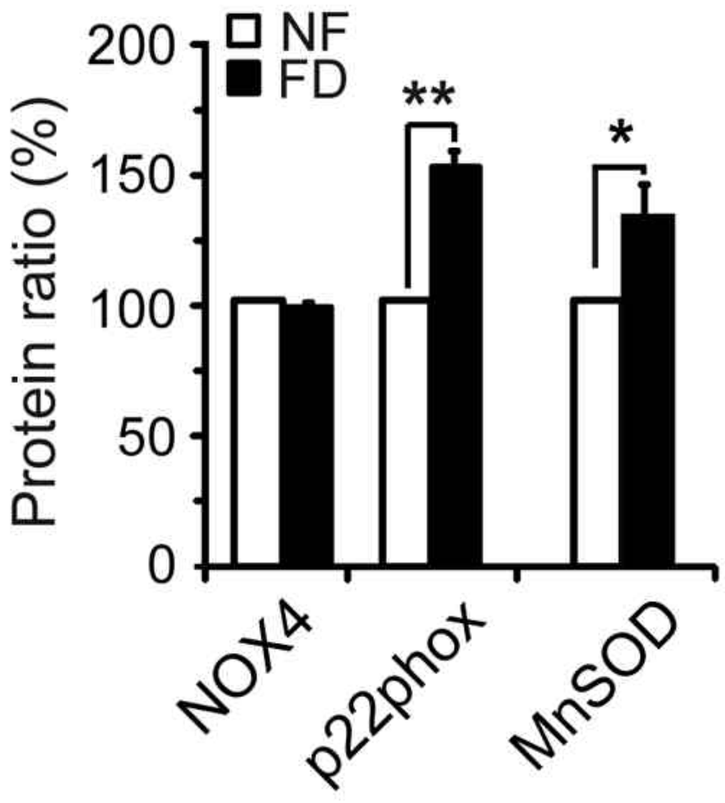
NF
FD
Protein ratio (%)
200
150
100
50
0
**
*
NOX4
p22phox
MnSOD

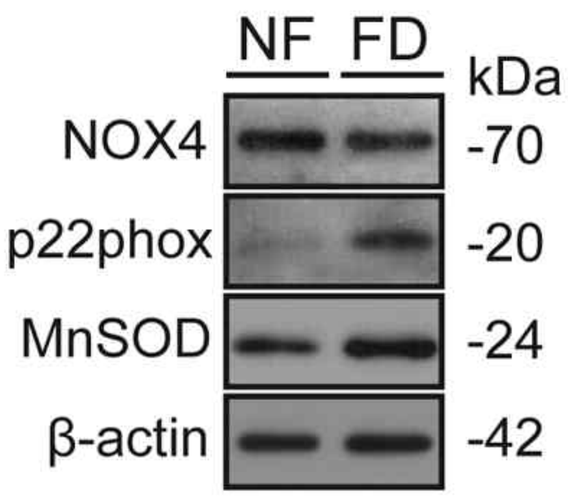
NF
FD
kDa
NOX4
-70
p22phox
-20
MnSOD
-24
β-actin
-42

C

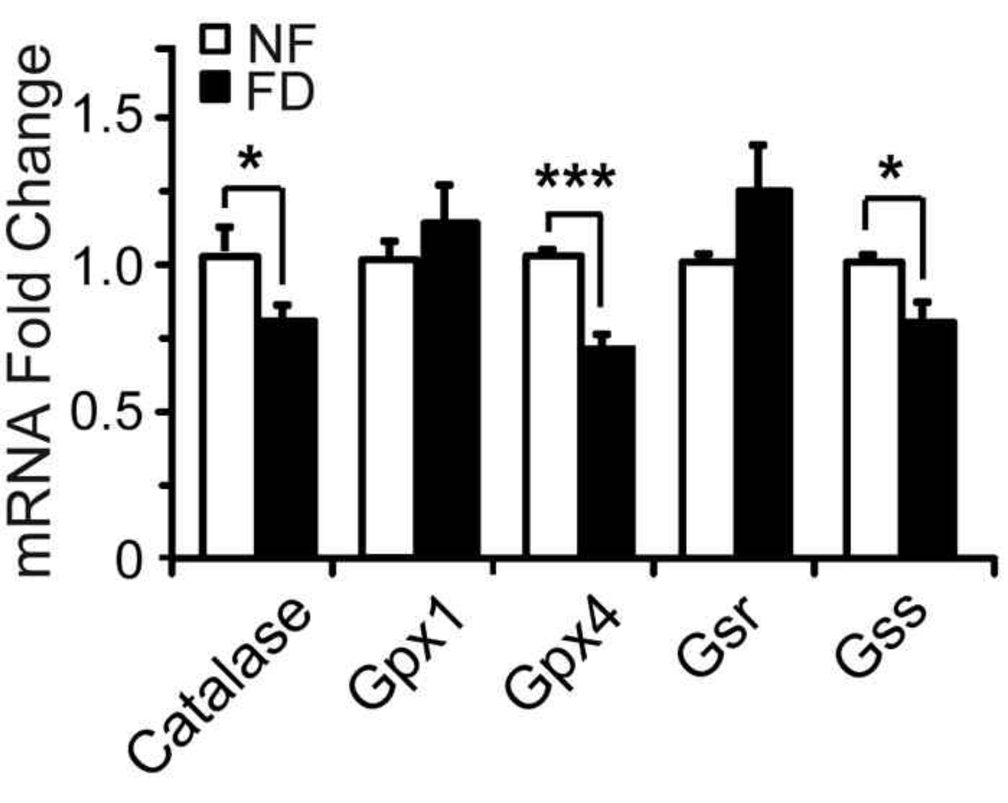
NF
FD
mRNA Fold Change
1.5
1.0
0.5
0
*
***
*
Catalase
Gpx1
Gpx4
Gsr
Gss

D

GSH
(pmol/mg protein)
8000
6000
4000
2000
0
**
NF
FD

GSSG
(pmol/mg protein)
800
600
400
200
0
***
NF
FD

E

a
b
3-NT
c
d
3-NT

e
3-NT staining intensity
200
150
100
50
0
NF
FD
***
***
StV
CG

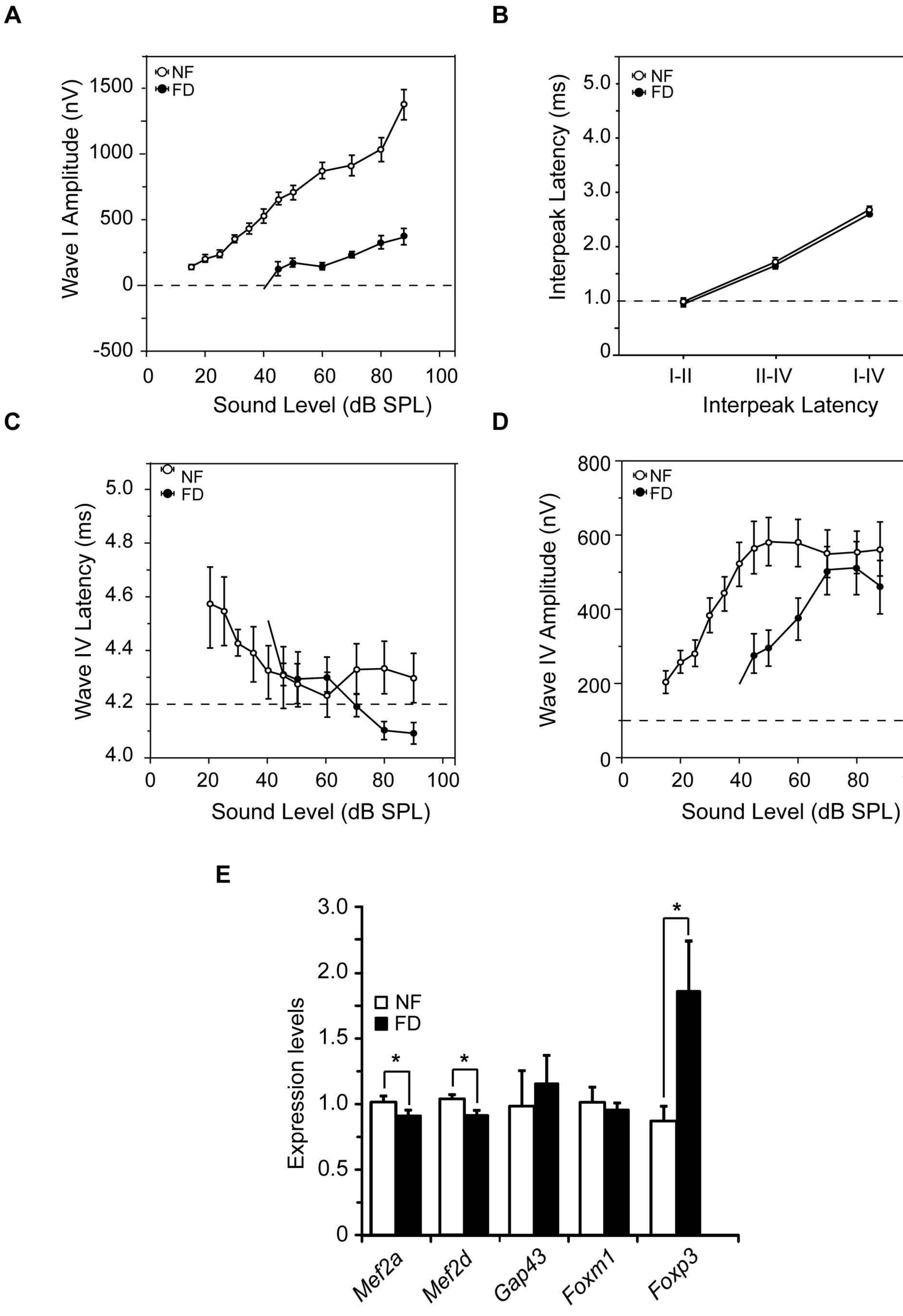

Figure S1. Click ABR interpreak latencies and input/output latency and amplitude plots for waves I and IV and gene expression of cochear markers. (A) Wave I amplitude-intensity plot (B) Click ABR interpeak latencies corresponding to I-II, II-IV and I-IV. (C) Wave IV latency-intensity graph (D) Wave IV amplitude-intensity graph. White circles represent the normal folate whilst black circles are used for the folate deficient mice (n=21 for each group). (E) *Mef2a, Mef2d, Gap43, Foxp3* and *Foxm1* expression in NF and FD mice using 18S and *Rplp0* genes as reference with similar results. Histograms show determinations made in triplicate for each animal sample in NF (n=6) and FD groups (n=6). Data were considered significant when p⊠ 0.05 (*). Data are shown as mean ± SEM.